

Development of Novel Polymeric Micellar DACHPt for Enhanced Platinum Based Chemotherapy in Colorectal Cancer

by

Abdulsalam Alharbi

A thesis submitted in partial fulfillment of the requirements for the degree of

Master of Science

In

PHARMACEUTICAL SCIENCES

Faculty of Pharmacy and Pharmaceutical Sciences
University of Alberta

© Abdulsalam Alharbi, 2018

ABSTRACT

One of the major limitations of chemotherapy in cancer treatment is the side effects of anti-cancer drugs. This happens due to non-selective distribution of most standard chemotherapies, and their action on cancer and all normal dividing cells. The objective of this project is to develop a novel delivery system for the more potent parent compound of oxaliplatin, dichloro (1,2-diaminocyclohexane) platinum(II) (DACHPt) to limit its non-selective distribution to normal tissues, thus reducing the drug's side effects. As an alternative to prodrug strategy, incorporation of DACHPt in polymeric micellar nanocarriers was hypothesized to increase DACHPt aqueous solubility and increase platinum delivery to colorectal cancerous tissues, while reducing platinum concentrations in normal tissues. Methoxy poly(ethylene oxide)-*block*-poly(α -carboxylate- ϵ -caprolactone) (PEO-*b*-PCCL) diblock copolymers were used to prepare micelles containing DACHPt through polymer-metal complex formation of DACHPt with PEO-*b*-PCCL (abbreviated as DACHPt-PCCL) in distilled water. The mean diameter of the prepared micelles was measured using dynamic light scattering (DLS) to be 60 nm. The release profile of DACHPt from DACHPt-PCCL micelles as measured by ICP-MS showed only 53.6% of platinum was released after 120 h from micelles compared to 96.5% platinum release from free drug at 7.5 h confirming drug complexation. The critical micelle concentration (CMC) and kinetic stability of DACHPt-PCCL micelles in the

presence of sodium dodecyl sulfate (SDS), studied using dynamic DLS. The results showed CMC at micromolar level and high kinetic stability for micelles in the presence of SDS implying micellar stability following dilution. DACHPt-PCCL micelles were able to increase the solubility of DACHPt from 0.25 mg/mL to 4.1 mg/mL (16 times) due to the high drug loading inside PEO-*b*-PCCL micelles (20 % w/w). The relative IC₅₀ of DACHPt-PCCL micelles against human colorectal cancer cell lines, HCT116, HT29 and SW620, as measured by MTT assay was higher than DACHPt; perhaps due to the slow release of platinum complexes from DACHPt-PCCL micelles and/or slower cell uptake. Free DACHPt showed higher cell uptake in HT29 cell line, and similar cell uptake in HCT116 and SW620 cell lines compared to DACHPt-PCCL micelles. The *in vivo* tissue distribution study in NIH-III mice bearing subcutaneous HCT116 tumors, 24 h following tail vein injection of DACHPt-PCCL micelles at a dose of 6 mg platinum/kg, showed higher platinum concentrations in plasma compared to animals injected with oxaliplatin, at the same platinum dose that led to a trending, but statistically non-significant increase in tumor platinum levels. Overall, our results point to a potential for DACHPt-PCCL micelles in delivery of DACHPt to colorectal cancer tissues.

Dedication

I dedicate this thesis to my beloved parents, Abdullah and Bakhita who have always been the main source of support and motivation; to my dear wife Rehab who has been in my side all the way with her support, patience and love; and to my little princess, Salma, who was always a source of happiness.

Acknowledgment

I would like to express my deepest gratitude to all of the following people.

- My supervisor Dr. Afsaneh Lavasanifar for her kindness, guidance, advice, and continuous support. I cannot thank her enough for her endless support and motivation throughout my studies.
- My supervisory committee members, Dr. Ayman El-Kadi and Dr. Raimar Löbenberg for their valuable comments, generous guidance and suggestions.
- Dr. Mohammed Reza Vakili for training me in the lab and his encouragements.
- Dr. Carlos A. Velázquez for accepting to be in my examination committee in such a short notice.
- My past and current lab mates for their help, support and fruitful discussions.
- Faculty staff, in particular, Ms. Joyce Johnson and Ms. Diseray Schamehorn for their support and help throughout the whole program.
- My beloved parents, brothers and sisters for their love, support and encouragement throughout my whole life.
- My dear wife, Rehab and my lovely daughter, Salma who accompanied me throughout the whole journey and supported me with their love and patience.
- Finally, I would like to thank the following institutions:
 - Umm-Alqura University, Mecca, Saudi Arabia, for providing me with my scholarship.
 - The Saudi Cultural Bureau in Canada, for managing my tuition fees and academic expenses.

- The Faculty of Pharmacy and Pharmaceutical Sciences, University of Alberta, Edmonton, Canada, for accepting me in the graduate studies program and providing me with the training, facilities and qualification.

TABLE OF CONTENTS

Chapter 1: Introduction	1
1.1 Platinum-based drugs.....	2
1.1.1 Cisplatin, the first platinum anticancer drug.....	2
1.1.1.2 Mechanism of action of cisplatin and its resistance mechanisms.....	4
1.1.2 Carboplatin and second-generation platinum-based drugs.....	6
1.1.3 Oxaliplatin and third-generation platinum-based drugs.....	7
1.1.4 New generation of platinum-based drugs.....	9
1.1.4.1 Platinum (IV) prodrugs.....	9
1.1.5 The role of carrier-based delivery in the improvement of platinum-based drugs.....	12
1.2 Polymeric micelles: an overview.....	13
1.3 Platinum-based drugs in polymeric micelles.....	15
1.4 Liposomal formulation of platinum-based drugs.....	16
1.5 Thesis proposal.....	17
1.5.1 Rational and significance.....	17
1.5.2 Hypothesis.....	19
1.5.3 Objective.....	19
1.5.4 Specific aims.....	19
Chapter 2: Experimental procedures	21
2.1 Materials.....	22
2.2 Methods.....	22

2.2.1 Synthesis of PEO-b-PBCL block copolymer.....	22
2.2.2 Synthesis of PEO-b-PCCL.....	23
2.2.3 Preparation of DACHPt polymeric micelles.....	24
2.2.4 Characterization of DACHPt polymeric micelles.....	25
2.2.5 In-vitro release study.....	26
2.2.6 In-vitro cytotoxicity studies.....	28
2.2.7 In-vitro cell uptake studies.....	29
2.2.8 <i>In vivo</i> Biodistribution study.....	30
2.2.8.1 Animals.....	30
2.2.8.2 Preparing HCT116 cells for inoculation.....	30
2.2.8.3 Subcutaneous tumor xenograft.....	30
2.2.8.4 Intravenous administration.....	31
2.2.8.5 Biodistribution study.....	31
2.2.8.6 Sample preparation for ICP-MS analysis.....	31
2.2.3 Statistical Analysis.....	32
Chapter 3: Results.....	33
3.1 Synthesis of PEO-b-PBCL block copolymer.....	34
3.2 Synthesis of PEO-b-PCCL.....	35
3.3 Preparation and characterization of DACHPt-PCCL polymeric micelles.....	37
3.4 <i>In vitro</i> release study.....	41
3.5 <i>In vitro</i> cytotoxicity studies.....	42
3.6 <i>In vitro</i> cell uptake studies.....	49
3.7. <i>In vivo</i> Biodistribution study.....	52

Chapter 4: Discussion and Conclusion	58
4.1 Discussion.....	59
4.1.1 Development of block copolymer based nanocarriers of DACHPt.....	59
4.1.2 Investigation of DACHPt release from DACHPt-PCCL micelles.....	63
4.1.3 <i>In vitro</i> cell studies.....	65
4.1.4. <i>In vivo</i> Biodistribution study.....	67
4.2 Conclusion.....	69
4.3 Future directions.....	71
References.....	73

List of Figures

Figure 1.1: Chemical structures of the clinically used platinum-based drugs.....	3
Figure 1.2: Scheme represents cisplatin mechanism of action and drug resistance.....	5
Figure 1.3: Chemical structures of some platinum(IV) prodrugs.....	11
Figure 1.4: The process of self-assembly for amphiphilic diblock copolymer.....	15
Figure 3.1: Chemical structure of PEO-b-PBCL (x = 114; y = 30).....	34
Figure 3.2: Chemical structure of PEO-b-PCCL (x = 114; y = 29).....	35
Figure 3.3: ¹ H NMR spectrum of PEO-PBCL(A) and PEO-b-PCCL (B).....	36
Figure 3.4: Scheme of DACHPt-PCCL micelles preparation and drug release mechanism in media containing chloride ion.....	38
Figure 3.5: Size distribution of DACHPt-PCCL micelles by DLS.....	39
Figure 3.6: Kinetic stability of DACHPt-PCCL micelles in presence of SDS by DLS. DACHPT-loaded micelles solution (concentration: 1mg/mL) was added to SDS solution (concentration: 6mg/mL) in 2/1 micelles/SDS ratio (n=3).....	40
Figure 3.7: The average size of DACHPt-PCCL micelles in presence of SDS by DLS. DACHPT-loaded micelles solution (concentration: 1mg/mL) was added to SDS solution (concentration: 40mg/mL) in 2/1 micelles/SDS ratio (n=3).....	40
Figure 3.8: Critical micellar concentration CMC of DACHPt-PCCL micelles by DLS (n=3)....	41
Figure 3.9: In-vitro release profile of DACHPt from DACHPt-PCCL micelles compared to free DACHPt in PBS (n=3).....	42
Figure 3.10: Cytotoxicity studies of DACHPt-PCCL micelles versus control treatments against HCT116 cell line after (A) 24 h, (B) 48 h and (C) 72 h (n=3).....	44
Figure 3.11: Cytotoxicity studies of DACHPt-PCCL micelles versus control treatments against SW620 cell line after (A) 24 h, (B) 48 h and (C) 72 h (n=3).....	46
Figure 3.12: Cytotoxicity studies DACHPt-PCCL micelles versus control treatments against HT29 cell line after (A) 24 h, (B) 48 h and (C) 72 h (n=3).....	48
Figure 3.13: Uptake of DACHPt-PCCL micelles versus free DACHPt by (A) HCT116, (B) SW620 and (C) HT29 cells at 5 and 24 hours. *Means statistically different (P<0.05), ns means statistically not different (P>0.05). Each bar represents mean cell uptake ± SD (n=3).....	51

Figure 3.14: Platinum accumulation in organs after 24 hours of injection of Oxaliplatin or DACHPt-PCCL micelles intravenously at a dose of 6 mg/kg on a platinum basis. *Means statistically different ($P < 0.05$), ns means statistically not different ($P > 0.05$). Each bar represents mean platinum accumulation \pm SD (n=3).....56

LIST OF TABLES

Table 1: Liposomal formulations of platinum-based drugs in clinical trials.....16

Table 3.1: The relative IC₅₀ of DACHPt-PCCL micelles and free DACHPt against HCT116, SW620 and HT29 cell lines after 24, 48 and 72 hours. *Means statistically different (P<0.05, students, t test), ** means statistically different (P<0.01, students, t test), **** means statistically different (P<0.0001, students, t test) Results are presented as mean ± SD, n=3.....48

Table 3.2: The ratio of tissue platinum concentration to the plasma platinum concentration (*K_p*) of oxaliplatin and DACHPt-PCCL micelles. * means statistically different (P<0.01, students, t test), ns means statistically not different (P>0.05, students' t test). Results are presented as mean± SD (n=3).....57

LIST OF ABBREVIATIONS

CTR1	Copper transporter 1
DACH	1,2-diaminocyclohexane
OCT1	Organic cation transporters 1
OCT2	Organic cation transporters 1
EPR	Enhanced permeability and retention
PEG	Poly(ethylene glycol)
PEO	Poly(ethylene oxide)
PEO-<i>b</i>-PLGA	PEO- <i>b</i> -poly (lactic- <i>co</i> -glycolic acid)
PEO-<i>b</i>-PDLLA	PEO- <i>b</i> -poly (D,L-lactic acid)
PEO-<i>b</i>-PLAA	PEO- <i>b</i> -poly(L-amino acids)
PEO-<i>b</i>-P(Asp)	PEO- <i>b</i> - poly(L-aspartic acid)
nm	Nanometer
BCL	α -Benzylcarboxylate- ϵ -caprolactone
PEO-<i>b</i>-PCCL	Poly (ethylene oxide)- <i>b</i> -poly-(α -carboxylate- ϵ -caprolactone)
PEO-<i>b</i>-PBCL	Poly (ethylene oxide)- <i>b</i> -Poly(α -benzyl- ϵ -caprolactone)
DP	Degree of polymerization
M_n	Number average Molecular weight
DLS	Dynamic light scattering
SDS	Sodium dodecyl sulfate
CMC	Critical Micellar Concentration

EE	Encapsulation efficiency
DL	Drug loading.
mL	Milliliter
IC₅₀	Fifty percent growth inhibitory concentration
uL	Microliter
mg	Milligram

CHAPTER ONE

INTRODUCTION

1.1 Platinum-based drugs

1.1.1 Cisplatin, the first platinum anticancer drug

Michele Peyrone was the first to synthesize cisplatin, *cis*-diamminedichloroplatinum(II) (Figure 1.1) in the end of nineteenth century, and it was known as Peyrone's chloride. In the late 1960s, the cisplatin's cytostatic property was discovered by Barnett Rosenberg while working on an experiment to investigate the effect of cisplatin on the growth of bacteria. Cisplatin has been approved by the US Food and Drug Administration for testicular and ovarian cancer in several countries in 1971 [1].

Cisplatin has an anticancer activity against different types of cancer, such as testicular, ovarian, head and neck, colorectal, bladder and lung cancer [2], [3]. Cisplatin usually have an initial therapeutic response and leads to complete cancer remission or cancer stabilization. However, it suffers from severe adverse effects including nausea and vomiting, ototoxicity as a result of the irreversible damage of the hair cells in Corti organ, peripheral sensory neuropathy, and dose limiting nephrotoxicity [4].

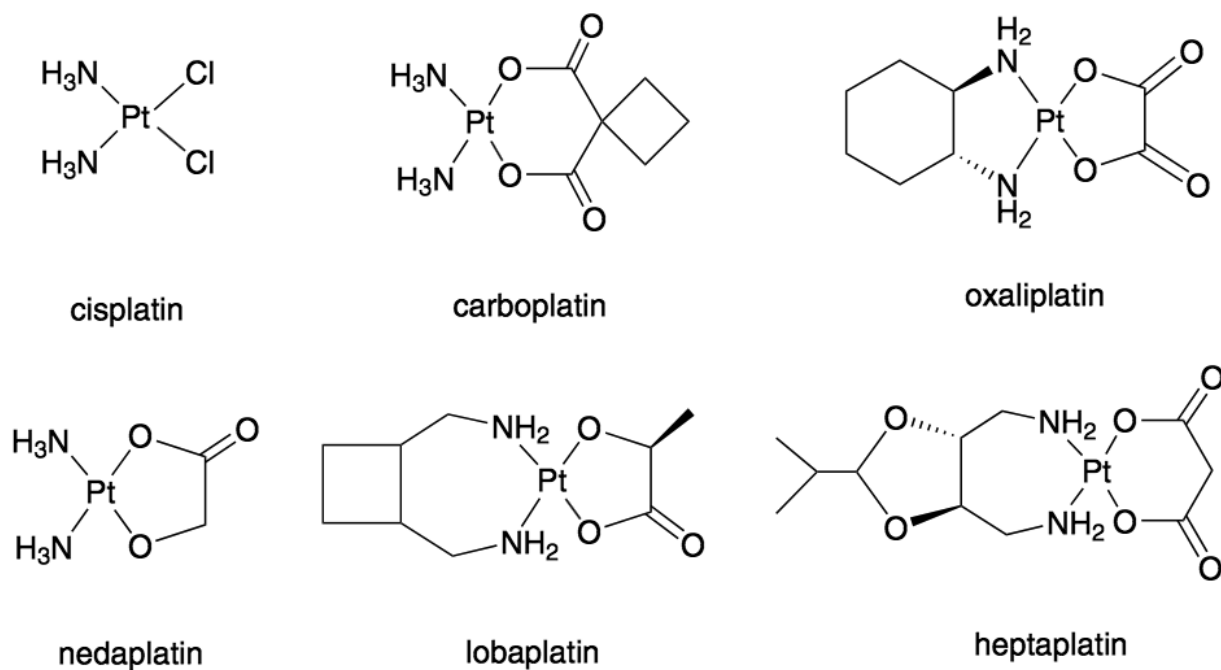


Figure 1.1: Chemical structures of the clinically used platinum-based drugs (Adapted from ref. 9 with permission).

Another obstacle limiting the effectiveness of cisplatin in cancer therapy is the development of cancer resistance. The resistance can be intrinsically to the platinum drugs or can be developed gradually after the therapy in several sensitive tumors [4].

1.1.1.2 Mechanism of action of cisplatin and its resistance mechanisms

Although DNA platination is considered as the main step in the cytotoxic effect of cisplatin, several other cellular steps have clear contribution in its effect. Any change in these cellular events may lead to drug resistance (Figure 1.2). Resistance mechanisms in cisplatin can be divided into pre-binding to DNA (due to cell uptake alterations or cytoplasmic degradation) and post-binding to DNA (due to pt-DNA lesions repairing [4]).

Cisplatin enters the cells mainly by passive diffusion and this cellular uptake mechanism is known to be both non-saturable as well as concentration-dependent. However, it has been found that extracellular methionine clusters of copper transporter 1 (CTR1) has a key role in the cellular uptake of cisplatin [5], [6]. CTR1 is an influx transporter of platinum and its downregulation was found in cisplatin-resistant cells [7]. CTR1 has a smaller molecular size than cisplatin, and studies suggest that before entering a cell, cisplatin is activated by interacting with CTR1, which results in the formation of an intermediate that is smaller than the radius of the narrowest opening of CTR1[6].

ATP7A and ATP7B are two other copper transporters that have a role in platinum resistance. ATP7A is thought to regulate platinum accumulation, primarily

by sequestering platinum intracellularly. However, ATP7B located in the Trans Golgi network mediates platinum drug efflux[6].

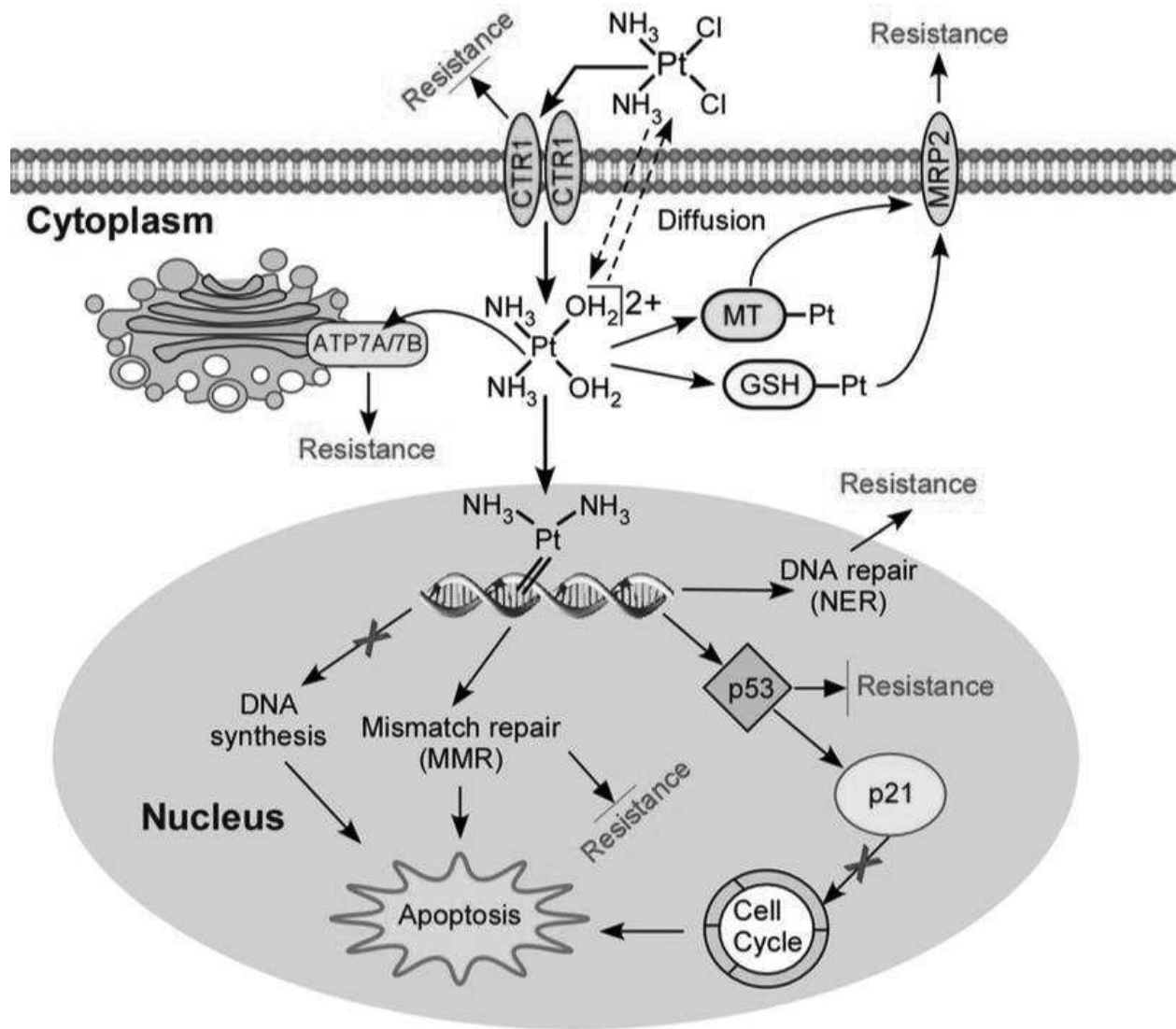


Figure 1.2: Scheme represents cisplatin mechanism of action and drug resistance (Adapted from ref. 9 with permission).

1.1.2 Carboplatin and second-generation platinum-based drugs

Carboplatin (the second-generation platinum drug) was developed to overcome the limitations and adverse effects of cisplatin (Figure 1.1). Carboplatin has similar mechanism of action to that of cisplatin. However, carboplatin and other second-generation platinum drugs have bidentate cyclobutane dicarboxylate ligands that make the aquation rate of these drugs lower than that of cisplatin [8]. Carboplatin showed lower neurotoxicity and ototoxicity compared to cisplatin because of the reduced aquation rate. Thus, carboplatin can be an appropriate choice for the aggressive tumors that need high-dose chemotherapy [9]. Carboplatin has been globally approved for ovarian cancer treatment, and it showed better activity in combination with paclitaxel compared to cisplatin [10]. However, carboplatin has dose-limiting toxicity such as myelosuppression, anemia, and neutropenia. Moreover, carboplatin showed lower activity than cisplatin in the treatment of testicular germ-cell cancers, bladder cancer, and head and neck cancer. Thus, cisplatin is still the first-choice drug for these diseases. Like cisplatin, several tumors have developed resistance against carboplatin, and this has limited its clinical use. Resistance mechanisms in carboplatin are similar to those reported for cisplatin [11].

Nedaplatin (cis-diammineglycolato platinum(II)) (Figure 1.1) has been developed with similar pharmacokinetic properties to cisplatin. Nevertheless, nedaplatin has improved the toxicity profile of cisplatin [9].

1.1.3 Oxaliplatin and third-generation platinum-based drugs

Oxaliplatin, a third-generation platinum-based drug (Figure 1.1), has been developed and showed lower resistance in cancer therapy compared to carboplatin and cisplatin. Oxaliplatin is given in combination with 5-fluorouracil and folinate for the treatment of metastatic and adjuvant colorectal cancer, which was insensitive to cisplatin [12]. Oxaliplatin has a leaving group of oxalate and it is a platinum complex with (1R,2R)-1,2-diaminocyclohexane (DACH) ligand. Due to the presence of bidentate oxalate, oxaliplatin has lower reactivity. Thus, the peripheral sensory neuropathy side effect was reduced in oxaliplatin [12]. The lipophilicity of DACH ligand in oxaliplatin increases its passive uptake compared to cisplatin and carboplatin. Moreover, this high lipophilicity gives an advantage to oxaliplatin to enter the cell by passive diffusion compared to cisplatin and carboplatin. It has been found that organic cation transporters (OCT1 and OCT2) have an important role in the cellular uptake of oxaliplatin as the overexpression of these transporters significantly increases the accumulation of oxaliplatin in the cells, but not

carboplatin or cisplatin. Organic cation transporters have overexpression in colorectal cancer cells which explain the efficacy of oxaliplatin in the treatment of this type of cancer [13]. In some clinical studies, after treatment with oxaliplatin, it has been found that the overexpression of OCT2 is correlated with increased survival of patients with metastatic colorectal cancer [14]. It has been found that downregulation of OCT1 is correlated with the developed resistance against oxaliplatin. Moreover, low expression of Na⁺/ K⁺-ATPase was found to be accompanied with resistance against oxaliplatin. Copper efflux transporters play a key role in the sensitivity of the cells to oxaliplatin, as well. Furthermore, better outcome was found in colorectal cancer patients with low levels of ATP7B, a copper efflux transporter [15].

Oxaliplatin binds to the DNA and forms crosslinks between guanine and adenine or on the guanine base (like cisplatin and carboplatin). However, oxaliplatin-DNA adducts inhibit the DNA synthesis more than cisplatin and carboplatin. This was attributed to the presence of the bulky and lipophilic DACH ligand in oxaliplatin. Clinical trials are evaluating oxaliplatin for the treatment of pancreatic, non-small lung, gastric, and breast cancers [12].

Other third-generation drugs, heptaplatin and lobaplatin have received regional approval (Figure 1). Lobaplatin was approved in China for the treatment of

myelogenous leukemia metastatic breast cancers [12]. It has thrombocytopenia as a dose-limiting side effect. Heptaplatin is very close to lobaplatin in the structure, however, it has a bulkier amine ligand. It has been developed to overcome the toxicity and the resistance accompanied with cisplatin. Heptaplatin is approved in Korea for treatment of gastric cancer. It has been shown in a phase III study that heptaplatin in combination with 5-fluorouracil has a comparable effect to that of cisplatin with 5-fluorouracil with lower hematological adverse effects [12].

1.1.4 New generation of platinum-based drugs

Despite the activity of the current approved platinum-based drugs in the treatment of different types of cancers, much efforts were applied to develop new platinum-based drugs with lower side effects and more sensitivity profile in different cancers. Several platinum complexes have been synthesized and investigated pre-clinically in cancer cells and tumor bearing animals. Some of these new platinum-based drugs have reached the clinical trials.

1.1.4.1 Platinum (IV) prodrugs

Platinum (IV) prodrugs have been developed to improve the pharmacological properties of the current in use platinum-based drugs (Figure 1.3). The new pharmacological properties of Platinum (IV) prodrugs are attributed to the addition

of ligands that can affect drug's physicochemical properties. The platinum (IV) prodrugs have shown higher stability in blood circulation as a result of increased interaction with plasma proteins. The activation of platinum (IV) prodrugs occurs after their reduction transforming them into different square planar platinum complexes. Although glutathione and ascorbate play an important role in the reduction of platinum (IV) prodrugs, most of the reduction happens by cellular proteins [16]. Platinum (IV) prodrugs have another advantage over the current platinum-based as they can be given orally due to their high stability as well as the reduced side effects. Therefore, platinum (IV) prodrugs seem to be a promising new class of anticancer drugs. Owing to new ligands used in their structure, they have potential in targeting the drug to the tumor. Thus, keeping these ligands attached to the platinum on the way to the tumor *in vivo* is essential. The ligand can then be cleaved off after reaching the tumor site. More studies are needed to understand the cellular accumulation mechanisms and biotransformation of these drugs in the bloodstream.

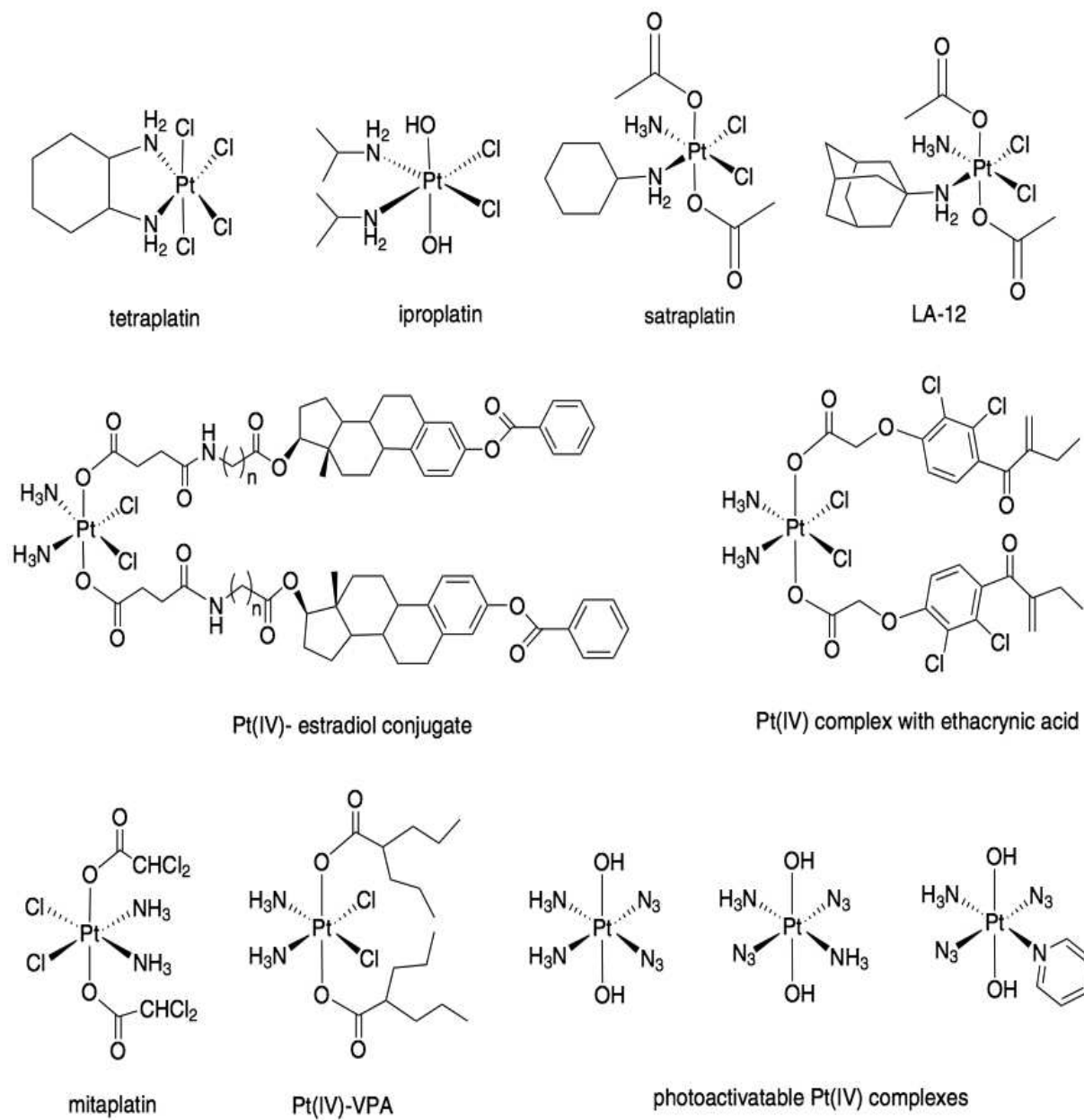


Figure 1.3: Chemical structures of some platinum(IV) prodrugs (Adapted from ref. 9 with permission).

1.1.5 The role of carrier-based delivery in the improvement of platinum-based drugs

Platinum-based drugs have brought significant advances in cancer therapy. However, their clinical use is limited by their adverse side effects as well as development of resistance. Moreover, most of these platinum-based drugs have low bioavailability and poor water solubility. Delivery of platinum drugs specifically to the tumor is an attractive strategy to overcome the limitations of these drugs that may potentially lead to improved drug activity, decreased drug resistance and lower adverse effects of platinum drugs. Drug delivery systems can be designed to increase drug accumulation levels in the tumor tissue, taking advantage of increase permeability and defective lymphatic clearance, as the so called enhanced permeability and retention (EPR) effect, in solid tumors [17]. Clinically used small molecule anticancer drugs can easily pass through normal and malignant vasculature and access different tissues, whereas nanoparticles delivery systems such as lipid-based nanoparticles, liposomes, polymeric micelles and other polymeric nanocarriers can bypass extravasation at tight continuous junctions of vasculature in normal tissue and accumulate passively in the tumor through preferred extravasation at leaky tumor vasculature. The nanoscale dimensions of these delivery systems are important to prevent their removal by renal clearance or extravasation in the normal tissues. The nanocarriers can also be modified on their surface with ligands against

receptors overexpressed by cancer cells to achieve higher selectivity, homing and entry to tumor cells [9].

Nanodelivery systems used for the encapsulation of anticancer drugs, usually bear a hydrophilic corona, such as a poly(ethylene glycol) (PEG) brush. Hydrated PEG has high water solubility, large exclusion volume and high mobility. Thus, it forms dense polymeric shield surrounding the nanoparticle protecting it from immune system recognition and opsonization [18].

1.2 Polymeric micelles: an overview

Polymeric micelles are carriers with core/shell structure and a diameter range of 10-100 nm [20–22]. Polymeric micelles can meet the requirements of a drug carrier in targeted drug delivery [22], [23]. Thus, they gained high attention as a platform for drug delivery in the last twenty years. Polymeric micelles can be formed in an aqueous media through self-assembly of amphiphilic block copolymers. In their core/shell structure, the hydrophobic part (core) acts as a reservoir for loading of hydrophobic drugs, DNA or proteins while the hydrophilic part (shell) interfaces the biological media (Figure 1.4) [24]. Polymeric micelles can circulate for prolonged time in the blood and accumulate selectively in the tumor due to the presence of the hydrophilic shell that make them able to escape opsonization and the uptake by phagocytic system like other stealth nanocarriers [26, 27]. The chemical

flexibility of the core/shell polymeric micelles structure is a unique characteristic that make them amenable for chemical manipulations and suitable to deliver wide range of drugs with different physicochemical properties and various modes of drug release. Moreover, polymeric micelles may be designed to have responsiveness to external or internal stimuli by interaction with specific targets, thus be used for active or physical drug targeting functions [22, 28, 29].

The most commonly used block copolymers in drug delivery include 1) PEO-*b*-poly(ester)s like PEO-*b*-poly (lactic-*co*-glycolic acid) (PEO-*b*-PLGA), PEO-*b*-poly (D, L-lactic acid) (PEO-*b*-PDLLA), and PEO-*b*-poly(ϵ -caprolactone) (PEO-*b*-PCL); 2) PEO-*b*-poly(L-amino acids) (PEO-*b*-PLAA) like PEO-*b*- poly(L-aspartic acid) (PEO-*b*-P(Asp)), PEO-*b*-poly(L-glutamic acid) (PEO-*b*-P(Glu)) and PEO-*b*-poly(L-lysine) (PEO-*b*-PLL); and 3) Poloxamers (Pluronic[®]) such as PEO-*b*-poly(propylene oxide)-*b*-PEO (PEO-*b*-PPO-*b*-PEO).

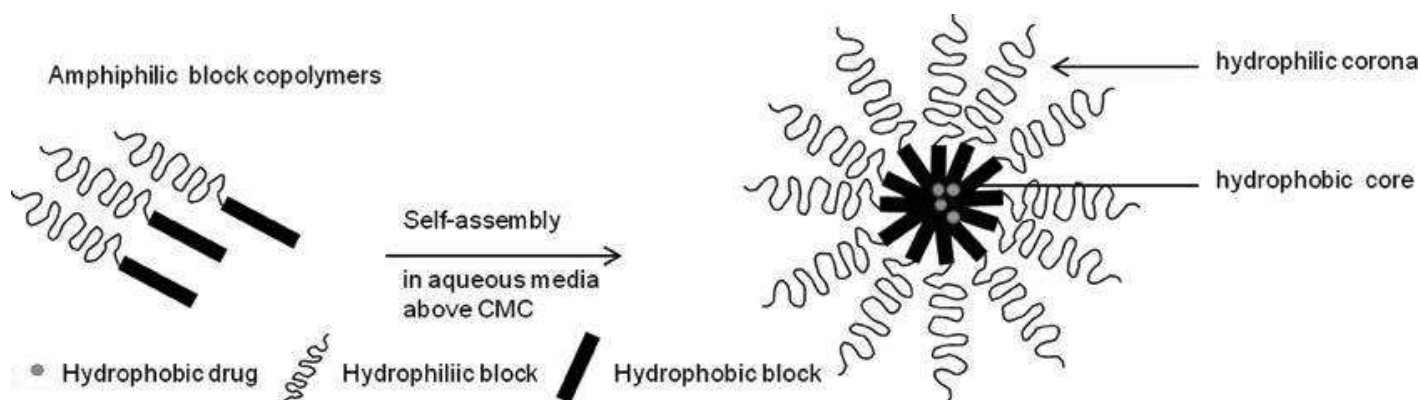


Figure 1.4: The process of self-assembly for amphiphilic diblock copolymer (Adapted from ref. 24 with permission).

1.3 Platinum-based drugs in polymeric micelles

After encapsulation of cisplatin in polymeric micelles, prolonged circulation of the drug in plasma, decreased nephrotoxicity and more accumulation of the drug in the tumor have been observed. With a size about 30 nm, cisplatin-loaded micelles can be penetrated even into poorly permeable tumors. NC-6004 or Nanoplatin is a PEO-PGlu-based cisplatin micelle formulation that has shown prolonged blood circulation as well as better tumor accumulation leading to full tumor regression in C26 tumor-bearing mice without significant weight loss [18].

NC-6004 has shown anticancer activity comparable to free cisplatin in mice inoculated with MKN-45 human gastric cells [29]. Phase I clinical trials of NC-6004 showed reduced adverse side effects and better tolerability compared to the free cisplatin [30]. NC-4016 is an oxaliplatin-loaded micelle formulation which have shown promising results, *in vivo*, in terms of overcoming oxaliplatin resistance. The clinical trials of NC-4016 are still under way [18].

In summary, development of nanodelivery systems for platinum-based drugs is an attractive way to overcome their limitations and increase their activity in resistant tumors. The chemical diversity of the delivery system may facilitate design of these new formulations.

1.4 Liposomal formulations of platinum-based drugs

Liposomes prepared from various amphiphilic phospholipids are lipid bilayer vesicles with an aqueous interior. The main advantage of this delivery system is that it can be used for both hydrophilic and hydrophobic drugs utilizing the aqueous cavity and phospholipid bilayer for drug accommodation, respectively [9]. Several platinum-based anticancer drugs encapsulated into liposomes have been investigated. So far, there are number of liposomal products for platinum anticancer drugs in clinical trials (Table 1) [9]. The major problem with liposomal formulations of platinum compounds is the very low drug release even at the site of drug action that has led to a significant reduction in drug potency.

Table 1: Liposomal formulations of platinum-based drugs in clinical trials.

Liposomal formulation	Platinum-based drug	Status
Lipoplatin	Cisplatin	Phase III
SPI-77	Cisplatin	Phase II
Aroplatin	cis- bis-(neodecanoato)- {(1R,2R)-1,2- diaminocyclohexane} platinum(II) (NDDP)	Phase II
Lipoxal	Oxaliplatin	Phase I

1.5 Thesis proposal

1.5.1 Rational and significance

The current anticancer drugs have low specificity and selectivity for the tumor cells. This leads to serious adverse effects of anti-cancer agents on normal cells. Nano drug delivery systems can have a great impact on limiting adverse effects of the encapsulated anticancer drugs by changing normal the biodistribution of these drugs away from normal tissues. The delivery systems are also expected to enhance (or at the least maintain) anti-cancer drug potency, *in vivo*, by increasing drug levels at the tumor site. nano-delivery systems of appropriate structure have the potential to improve the therapeutic index of anticancer drugs through an increase in their toxic dose and/or a reduction in their effective dose.

Cisplatin, the first generation of platinum-based drug suffers from serious dose-related adverse effects (such as neurotoxicity, ototoxicity, nausea and vomiting, and nephrotoxicity) as well as development of intrinsic and acquired resistance [31] . Several research investigations have been devoted to developing new analogs of cisplatin. Among these analogs, dichloro (1,2-diaminocyclohexane) platinum(II) (DACHPt) is a compound which has shown remarkable and wide spectrum activity in different cancers, lower adverse effects with no cross resistance in many cisplatin-resistant cancers [12, 33–36]. However, DACHPt has much lower

solubility in water compared to cisplatin. Oxaliplatin has been developed to increase the water solubility of DACHPt.

Although oxaliplatin showed better tolerability compared to other platinum-based drugs, some adverse effects, such as neurotoxicity and acute dysesthesias, still limits the range of its working doses [36]–[39]. Many drug delivery systems have been developed to improve oxaliplatin therapeutic index through affecting drug's pharmacokinetics and biological disposition [40]–[45]. Development of polymeric micelles complexed with DACHPt could lead to an oxaliplatin carrier with modified pharmacokinetics and/or higher tumor accumulation. NC-4016 is a micellar formulation that have reached clinical trials and prepared from complexation of DACHPt with PEG-poly(glutamic acid). NC-4016 was able to increase $AUC_{0-72\text{ h}}$ of DACHPt in plasma and tumor 1000 and 17 times, respectively, when compared to oxaliplatin. Moreover, NC-4016 showed higher activity against metastatic disease over oxaliplatin in various tumor models [46]. However, development of polyester-based micellar delivery system for oxaliplatin could show a better safety profile when compared to poly(amino acid) based polymeric micelles. Polyesters have a history of safe application as absorbable sutures and drug delivery systems in humans [21].

1.5.2 Hypothesis

Polymeric DACHPt micelles based on PEO-PCCL-DACHPt complex can increase DACHPt aqueous solubility to clinical relevant concentrations for intravenous administration, hold on to their drug content, and modify platinum disposition, away from normal tissue and towards blood circulation and tumor in colorectal cancer *in vivo* models.

1.5.3 Objective

The objective of this project is to develop a novel delivery system for the more potent parent compound of oxaliplatin, dichloro (1,2-diaminocyclohexane) platinum(II) (DACHPt) to limit its non-selective distribution to normal tissues, thus reducing the drug's side effects.

1.5.4 Specific aims

Towards this long-term objective, the following specific aims were pursued in this thesis:

- 1- Development of a novel polymeric micellar formulation for DACHPt delivery based on its complexation with PEO-PCCL.

- 2- Characterization of this formulation for its average diameter, platinum loading, *in vitro* release profile and stability.
- 3- Assessment of the effect of DACHPt micelles on *in vitro* cytotoxicity and uptake by human colorectal cancer cells compared to the free drug.
- 4- Assessment of the effect of DACHPt micelles on the *in vivo* biodistribution of platinum in a subcutaneous colorectal cancer model compared to oxaliplatin.

CHAPTER TWO
EXPERIMENTAL PROCEDURES

2.1 Materials

Dichloro(1,2-diaminocyclohexane)platinum(II) (DACHPt), methoxy poly(ethylene glycol) (PEG) (Mn 5000 Da, purity 99.99%), palladium-coated charcoal were purchased from Sigma (St. Louis, MO, USA). α -Benzylcarboxylate- ϵ -caprolactone monomer (BCL) was custom synthesized by Alberta Research Chemicals Inc. (ARCI, Edmonton, AB, Canada). Stannous octoate was purchased from MP Biomedicals Inc., Tuttingen, Germany. M-PER mammalian protein extraction reagent and Micro BCA protein assay kit were purchased from Fisher Scientific. All other reagents were of analytical grade. HCT116, SW620, and HT29 human colorectal cell lines were obtained as a generous gift from the laboratory of Dr. Michael Weinfeld. Female NIH-III immune-deficient mice were purchased from Charles River Laboratories, USA.

2.2 Methods

2.2.1 Synthesis of Poly(ethylene oxide)-*b*-Poly(α -benzyl- ϵ -caprolactone) (PEO-*b*-PBCL) block copolymer

The synthesis of PEO-*b*-PBCL was previously reported by our research group [21]. Briefly, PEO-*b*-PBCL was first synthesized by ring opening polymerization of BCL (0.7g, 2.8 mmol) using methoxy PEO (Mw: 5000 Da, 0.6 g, 0.12 mmol) as initiator and stannous octoate (0.002eq. of monomer) as a catalyst in 10 mL ampule.

The ampule was sealed under vacuum, then the polymerization reaction was allowed to proceed for 4 h at 140 °C in oven. Then, the product was cooled to room temperature to terminate the reaction. The prepared PEO-*b*-PBCL was characterized using ¹H NMR (Bruker, ASENDTM 600 MHz spectrometer) in deuterated chloroform (CDCl₃) at 600 MHz at room temperature. The degree of polymerization (DP) and the number average molecular weight (M_n) of the block copolymers were calculated by comparing peak intensity of -O-CH₂- (δ= 4.17 ppm) for α-benzyl carboxylate-ε-caprolactone to the intensity of the same peak for PEO (δ= 3.65 ppm) in the ¹H NMR spectrum of PEO-*b*-PBCL.

2.2.2 Synthesis of PEO-*b*-PCCL

PEO-*b*-PCCL was synthesized by complete catalytic debenzylation of PEO-*b*-PBCL in the presence of hydrogen gas using palladium-coated charcoal. PEO-*b*-PBCL solution was dissolved in 100 mL of degassed tetrahydrofuran in 250 mL bottle, and charcoal-coated palladium (100 mg) was then dispersed into the solution. Hydrogen gas cylinder was connected to the bottle, and the solution was stirred using a magnetic stirrer at room temperature for 12 hours. After that, the mixture was centrifuged at 3000 rpm to remove the catalyst. The supernatant was collected, and pure polymer was precipitated into diethyl ether and washed repeatedly to remove impurities. Then, the final product was collected and dried under vacuum for 24 h at

room temperature. The prepared PEO-*b*-PCCL was characterized for its number average molecular weight by ^1H NMR (Bruker) using CDCl_3 as a solvent at room temperature.

2.2.3 Preparation of DACHPt polymeric micelles

Dichloro(1,2-diaminocyclohexane)platinum(II) DACHPt (40 mg, 0.0001M) was reacted with silver nitrate (18 mg, 0.0002M), ($[\text{AgNO}_3]/[\text{DACHPt}]=2$) in water for 24 hours at room temperature in the dark to form the aqueous complex. To eliminate AgCl precipitates, the mixture was centrifuged at 3000 rpm for 10 min. Then, the supernatant was purified by passage through a 0.22- μm filter. PEO-*b*-PCCL (8.24 mg) was dissolved in 2 mL of *N,N*-dimethylformamide (DMF), and this solution was added to the solution of DACHPt aqueous complex ($[\text{DACHPt}]/[\text{PCCL}]=14$) and reacted for 120 h at 37 $^\circ\text{C}$ to prepare DACHPt-PCCL conjugates. DACHPt-PCCL micelles were prepared by dialysis method. For this purpose, DACHPt-PCCL conjugates solution were placed into a dialysis bag (Spectrapor, MWCO 3500) and dialyzed against water at 4 $^\circ\text{C}$ for 24 hours and the media was replaced with fresh one, several times to remove DMF and free DACHPt.

2.2.4 Characterization of DACHPt polymeric micelles

The size distribution of DACHPt-complexed micelles was evaluated by dynamic light scattering (DLS) measurement at 25 C° using Malvern Zetasizer (Nano ZEN 3600, Malvern, UK). The kinetic stability of micelles was also studied in the presence of sodium dodecyl sulfate (SDS) as a destabilizing agent using dynamic DLS (Malvern Zetasizer, Nano ZEN 3600) by studying the time-dependent changes in the relative scattered light intensity (intensity of scattered light at time t /intensity of scattered light at time zero) of DACHPT-PCCL micelles. DACHPT-PCCL micellar solution (concentration: 1 mg/mL) was added to SDS solution (concentration: 40 mg/mL) in 2:1 micelles:SDS ratio. The resulting mixture was then monitored using DLS for several time intervals. The mean intensity diameter of the DACHPT-loaded micelles was measured by DLS at the same time points.

Critical Micellar Concentration (CMC) of PEO-*b*-PCCL before and after complexation of DACHPt was determined by DLS measurement at 25 C° using Malvern Zetasizer (Nano ZEN 3600, Malvern, UK). A series of polymer concentrations (0.002 to 1.5 mg/mL) were prepared in deionized water. The average intensity of scattered light from three measurements was plotted against polymer concentration, and the CMC value was defined as the intersection of the two linear

lines in the sigmoidal curve, which reflect the onset of a rise in the intensity of scattered light.

The platinum content in the micelles was determined by ion coupled plasma-mass spectrometry (ICP-MS, Agilent Technologies, Tokyo, Japan). The encapsulation efficiency (EE) and drug loading (DL) percentages were calculated using the following equations:

Encapsulation efficiency EE (%)

$$\frac{\text{Amount of DACHPt complexed by polymeric micelles in mg determined by ICP-MS}}{\text{Amount of DACHPt initially added in mg}} \times 100$$

DACHPt loading percentage (%) (w/w)

$$\frac{\text{Amount of DACHPt complexed by polymeric micelles in mg determined by ICP-MS}}{\text{The total amount of the polymer in mg}} \times 100$$

2.2.5 *In vitro* drug release study

The release of DACHPt from micelles was evaluated using equilibrium dialysis method. DACHPt-micelles solution (2 mL) or free DACHPt solution (2 mL) with the same DACHPt content were placed into a dialysis bag (Spectraphor, Mw

cutoff 3500 g/mol) and dialyzed against phosphate buffered saline (PBS, pH 7.4; 0.14M NaCl; 1000 mL) at 37 C° in a Julabo SW 22 shaking water bath (Seelbach, Germany). At selected time intervals, 100 µL was collected from inside the dialysis bag and replaced with fresh one. The 1000 mL PBS in the recipient media was taken out and replaced by fresh PBS at the same time interval to maintain sink condition. Platinum content was determined by ICP-MS. For samples collected from DACHPt micelles, 60 % HNO₃ was added to the samples in a ratio of 1:1 to digest the micelles, then samples were analyzed for platinum content using ICP-MS. The remaining platinum concentration was subtracted from the initial concentration of the platinum and used to plot the cumulative drug release (%) versus time. The release profiles were compared using similarity factor, f_2 , and the profiles were considered significantly different if $f_2 < 50\%$.

The similarity factor, f_2 , was calculated based on the following Equation:

$$f_2 = 50 \times \log \left\{ \left[1 + (1/n) \sum_{j=1}^n (R_j - T_j)^2 \right]^{-\frac{1}{2}} \times 100 \right\}$$

where n is the sampling number, R_j and T_j are the percent released of the reference and test formulations at each time point.

2.2.6 *In vitro* cytotoxicity studies

Cell culture

HCT116, SW620, and HT29 human colorectal cell lines were obtained as a generous gift from the laboratory of Dr Michael Weinfeld and cultured in DMEM–Dulbecco's Modified Eagle Medium with 10% fetal bovine serum (Invitrogen, Karlsruhe, Germany) and 1% streptomycin-penicillin in a humidified incubator under 95% air and 5% CO₂ at 37 C°.

The relative fifty percent growth inhibitory concentration (IC₅₀) of free DACHPt and DACHPt-loaded micelles against HCT116, SW620, and HT29 human colorectal cell lines was evaluated by measuring the extent of reduction of MTT (3-(4,5-dimethylthiazol-2-yl)-2,5-diphenyltetrazolium bromide (Sigma–Aldrich, Oakville, ON, Canada) to formazan crystals. HCT116, SW620, and HT29 cells (1 x 10³ cells/well 100 µL) were seeded in separate 96-well plates in DMEM media containing 10% fetal bovine serum and incubated overnight and then exposed to increasing concentration of DACHPt (3.32-332 µM) in a free or DACHPt-loaded micelle form as well as plain micelles (n=3) for 24, 48, and 72 hours. After 24, 48, or 72 h, MTT solution (5 mg/mL 20 uL) was added to each well, followed by incubation for another 2 h at 37 C°. Finally, the medium was aspirated and 200 µL of N,N, dimethyl sulfoxide (DMSO) was added to dissolve the crystals formed, then

the absorbance was read at the wavelength of 570 nm using a plate reader (Synergy H1 Hybrid Reader, Biotek). The IC₅₀ was calculated from the plot of the % of viable cells versus log DACHPt concentration.

2.2.7 *In vitro* cell uptake studies

Cellular uptake of DACHPt was quantified by ICP-MS. HCT116, SW620, and HT29 (0.7 x 10⁶/flask) were seeded in 25 cm² flasks overnight. Cells were exposed to free DACHPt or its micellar formulation (50 μM) for 4 and 24 hours. Afterwards, the medium was aspirated, cells were rinsed with cold PBS, detached using trypsin-EDTA and pelleted by centrifugation at 300 x g for 5 minutes. Cell pellets were lysed using M-PER™ Mammalian Protein Extraction Reagent and quantified for protein content using the BCA protein assay kit (Pierce, Rockford, IL, USA). The remaining amount was digested with 60 % (v/v) HNO₃ overnight at 60 C° and analyzed for platinum (II) content by ICP-MS. The cell uptake is expressed as ng platinum/mg cell protein.

2.2.8 *In vivo* biodistribution study

2.2.8.1 Animals

Female NIH-III immune-deficient mice were purchased from Charles River Laboratories. All animals were housed in a pathogen free room upon arrival for at least a week prior to the study. The animal study was conducted under direct supervision of Health Sciences Laboratory Animal Services (HSLAS), University of Alberta and performed according to the guidelines approved by Canadian Council of Animal Care (CCAC). Free access to water and food was permitted prior to experimentation.

2.2.8.2 Preparing HCT116 cells for inoculation

HCT116 cells were cultured in three 75 cm² flasks to obtain enough number of cells for inoculation. At the day of injection, cells were harvested and mixed with Matrigel and media (1:1 ratio) to facilitate tumor formation and growth.

2.2.8.3 Subcutaneous tumor xenograft

NIH-III mice were divided into two groups (n=3) and inoculated subcutaneously in the right flank with HCT 116 cells (0.5×10^6). Mice were left until the tumor reached appropriate size for excision (21 days).

2.2.8.4 Intravenous administration

After 21 days, oxaliplatin and DACHPt-loaded micelles were administered intravenously in the tail vein at a dose of 6 mg/kg on a platinum basis.

2.2.8.5 Biodistribution study

After 24 hours of injection of oxaliplatin and DACHPt-loaded micelles, the mice were euthanized, and the blood was collected from the inferior vena cava, heparinized, and centrifuged to obtain the plasma. The plasma was kept at -20 C° until analysis. The tumor, liver, spleen, kidneys, heart, brain and lung were excised and stored at -80 C° until analysis.

2.2.8.6 Sample preparation for ICP-MS analysis

One hundred uL of plasma was digested in 300 uL of 60% HNO₃ at 56 °C overnight. 30-110 mg of each tissue (tumor, heart, spleen, kidney, lung, brain and liver) was homogenized in 2 mL of water, then 6 mL of 60 % HNO₃ was added for digestion at 56 C° overnight. The platinum concentration in the plasma and all tissues was determined by ICP-MS. Also, the ratio of tissue platinum concentration to the plasma platinum concentration (K_p) of oxaliplatin and DACHPt micelles were calculated.

2.2.3 Statistical Analysis

Compiled data are presented throughout the thesis as mean \pm standard deviation (SD). The data were analyzed for statistical significance by unpaired Student's t-test. Similarity test (f_2) was used as a statistical test to compare two release profiles.

CHAPTER THREE

RESULTS

3.1 Synthesis of PEO-*b*-PBCL block copolymer

The PEO-*b*-PBCL block copolymer was synthesized by ring-opening polymerization of α -benzyl carboxylate- ϵ -caprolactone using PEO as an initiator and stannous octoate as a catalyst (Figure 3.1). The molecular weight of PEO-*b*-PBCL copolymer was calculated using ^1H NMR by comparing peak intensity of -O-CH₂- (δ = 4.17 ppm) for α -benzyl carboxylate- ϵ -caprolactone to the intensity of the same peak for PEO (δ = 3.65 ppm) to be 12.6 kg/mol, corresponding to an average degree of polymerization of 31 for BCL (Figure 3.3).

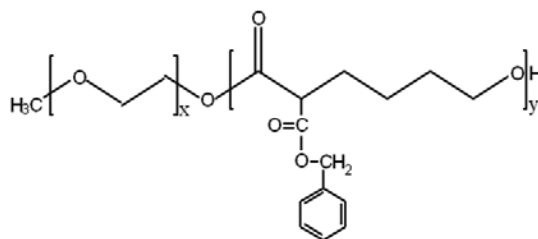


Figure 3.1: Chemical structure of PEO-*b*-PBCL ($x = 114$; $y = 30$).

3.2 Synthesis of PEO-*b*-PCCL

PEO-*b*-PCCL block copolymer (Figure 3.2) was synthesized through reduction of benzyl carboxylate on the PEO-*b*-PBCL block copolymer. The molecular weight of prepared PEO-*b*-PCCL was calculated by comparing peak intensity of -O-CH₂- (δ = 4.17 ppm) for α -benzyl carboxylate- ϵ -caprolactone to the intensity of the same peak for PEO (δ = 3.65 ppm) in the ¹H NMR spectrum to be 10.056 kg/mol. This would correspond to a degree of polymerization of 30 for the PCCL. The absence of benzyl protons at 5.2 ppm and aromatic peaks at 7.3 ppm was used as an indicator of the complete reduction of PBCL block (Figure 3.3).

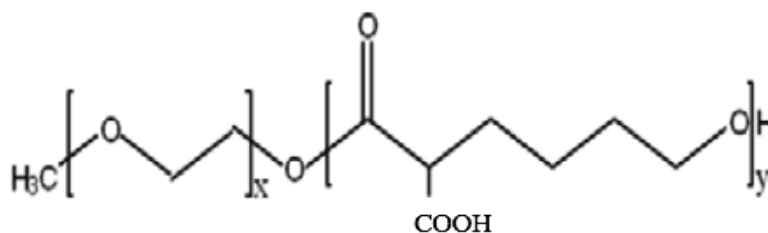
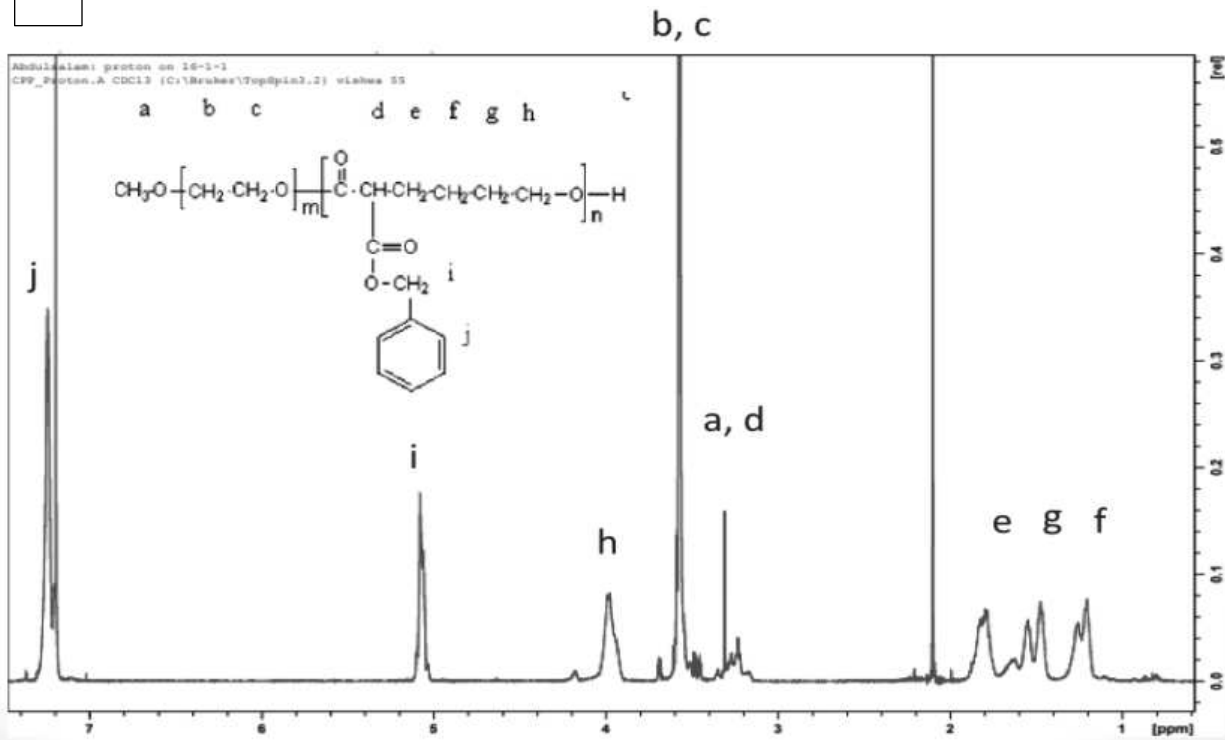


Figure 3.2: Chemical structure of PEO-*b*-PCCL ($x = 114$; $y = 29$).

A



B

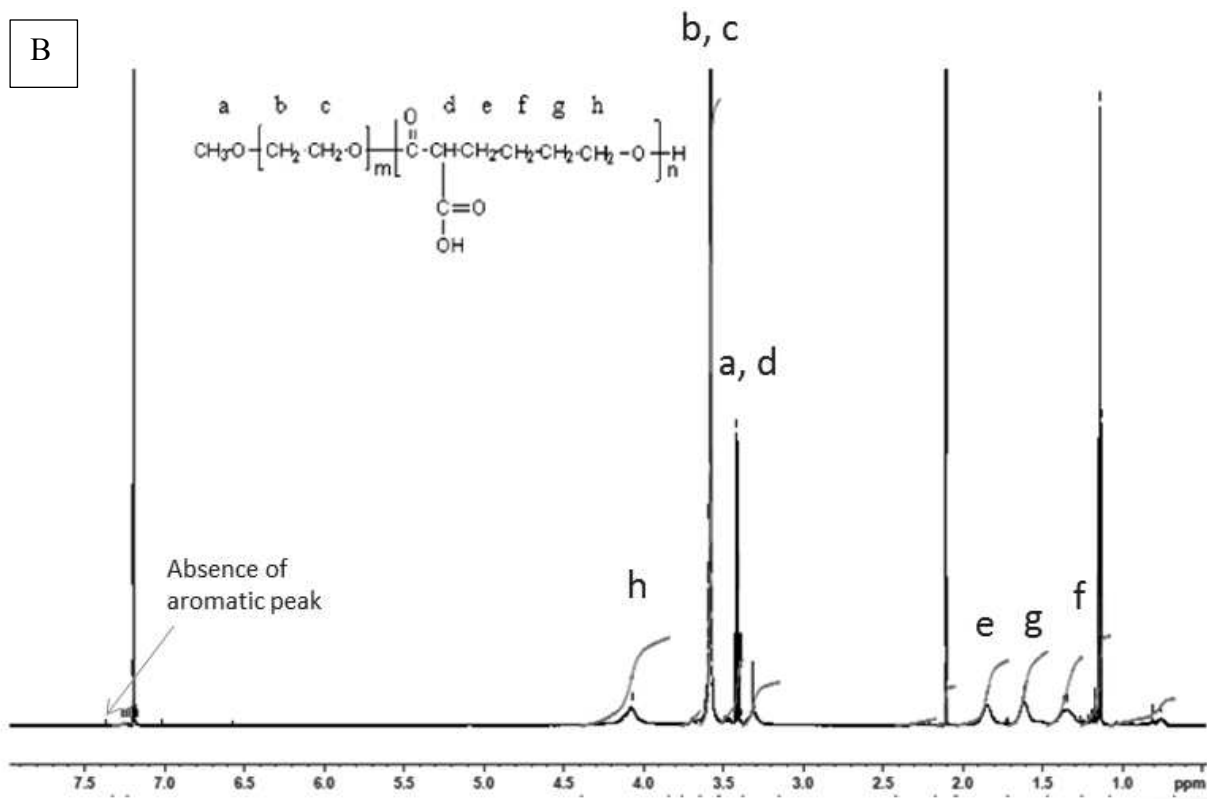


Figure 3.3: ¹H NMR spectrum of PEO-b-PBCL(A) and PEO-b-PCCL (B).

3.3 Preparation and characterization of DACHPt polymeric micelles

DACHPt-PCCL micelles were prepared through metal ion complex formation between DACHPt and the carboxyl ion of the PCCL block followed by self-assembly of PEO-*b*-PCCL/DACHPt complexes to polymeric micelles (Figure 3.4). The average diameter of DACHPt-PCCL micelles at [DACHPt]/[PCCL] of 14 was determined using dynamic light scattering (DLS) technique was 60 nm (Figure 3.5). DACHPt-PCCL micelles showed high encapsulation efficiency EE of 50% and drug loading DL of 20% (w/w). DACHPt has a very poor water solubility (0.25 mg/mL). DACHPt-PCCL micelles were able to increase DACHPt solubility to 4.1 mg/mL (i.e. 16 times higher).

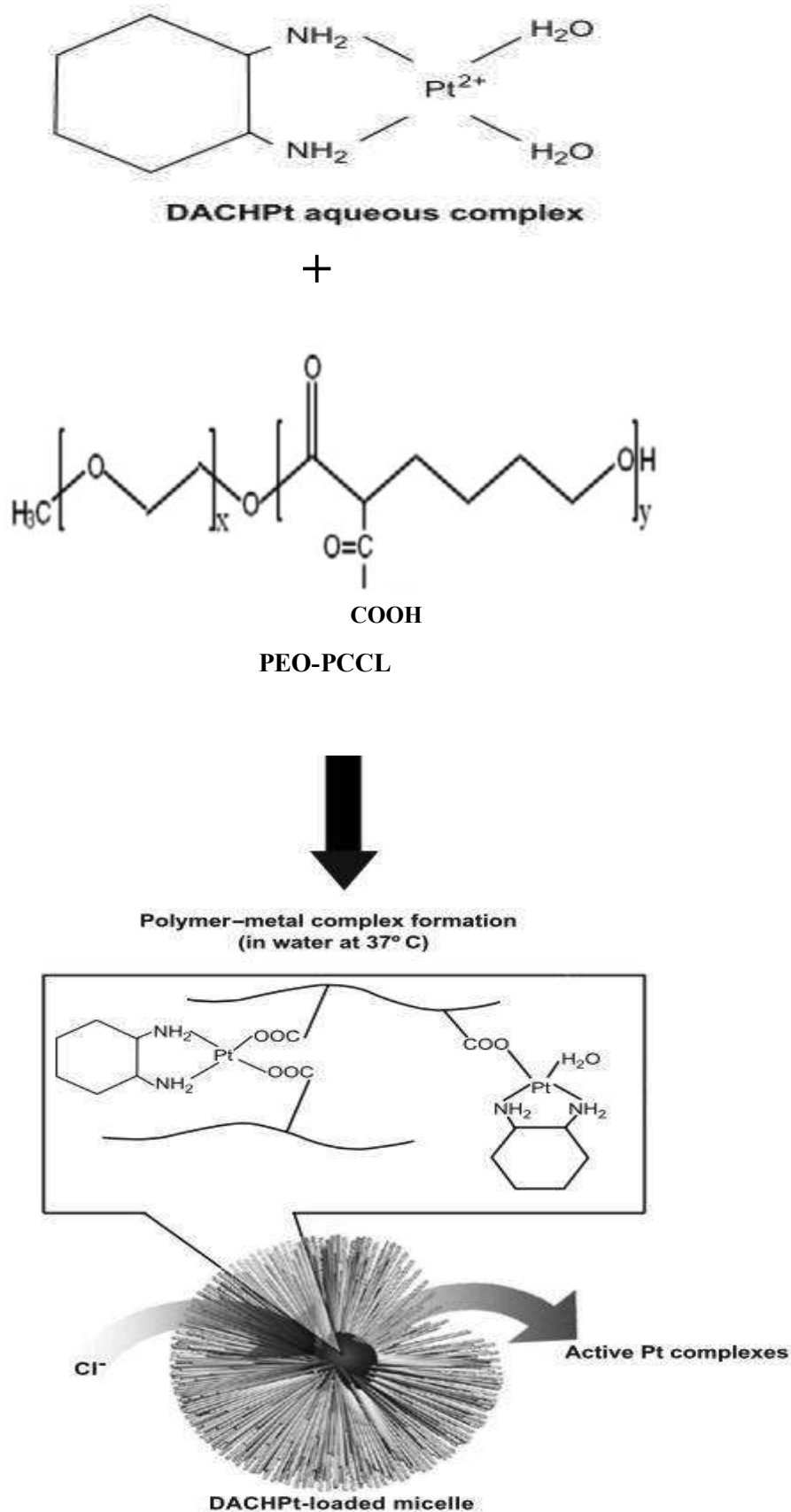


Figure 3.4: Scheme of DACHPt micelles preparation and drug release mechanism in media containing chloride ion (Adapted from ref. 31 with modification).

DACHPt-PCCL micelles showed high stability in the presence of SDS as a destabilizing agent and maintained their intensity for 10 days as determined by DLS technique (Figure 3.6). Moreover, DACHPt-PCCL micelles were able to maintain their mean diameter size for 10 days. (Figure 3.7).

The CMC of DACHPt-PCCL and plain micelles were determined by DLS measurement at 25 C° and found to be 8.9×10^{-6} and 3.6×10^{-5} μM , respectively (Figure 3.8). The scattering intensities detected for DACHPt-PCCL micelle concentrations below CMC have an approximately same value. The intensity starts to show a linear increase with concentration at the CMC, as the number of micelles increases in the solution.

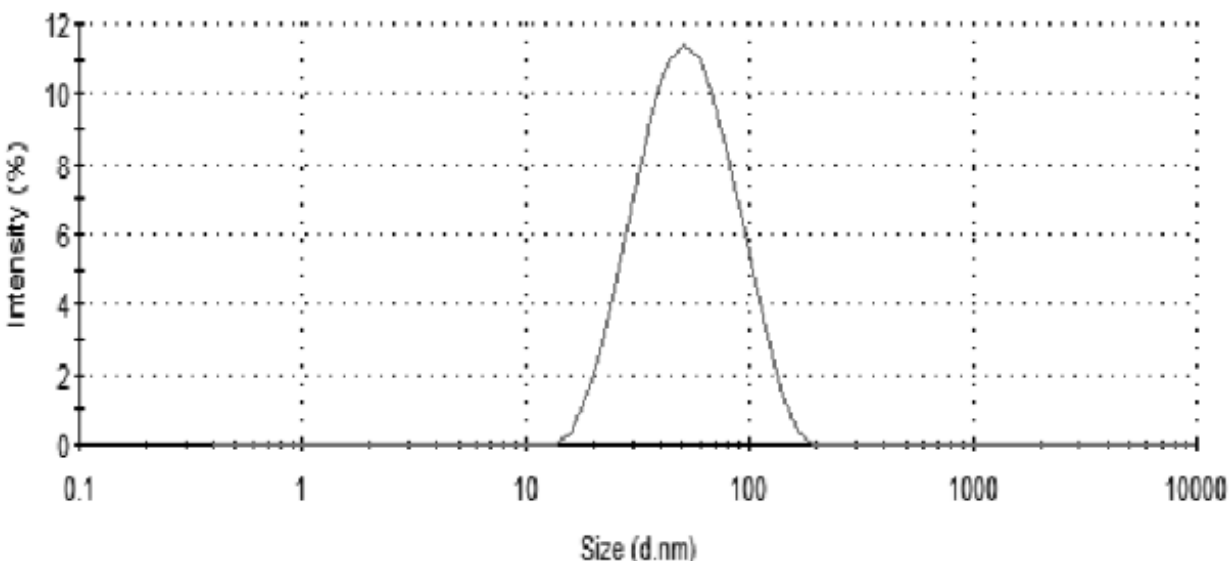


Figure 3.5: Size distribution of DACHPt-PCCL micelles by DLS.

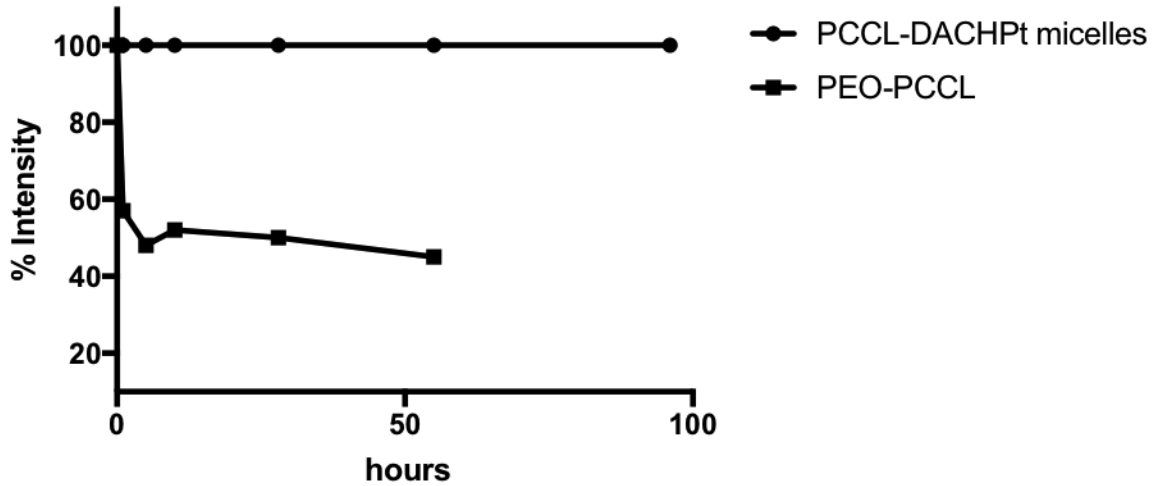


Figure 3.6: Kinetic stability of DACHPt-PCCL micelles and plain PEO-PCCL micelles in the presence of SDS by DLS. DACHPt-PCCL micelles solution (concentration: 1mg/mL) was added to SDS solution (concentration: 6 mg/mL) in 2:1 micelles:SDS ratio.

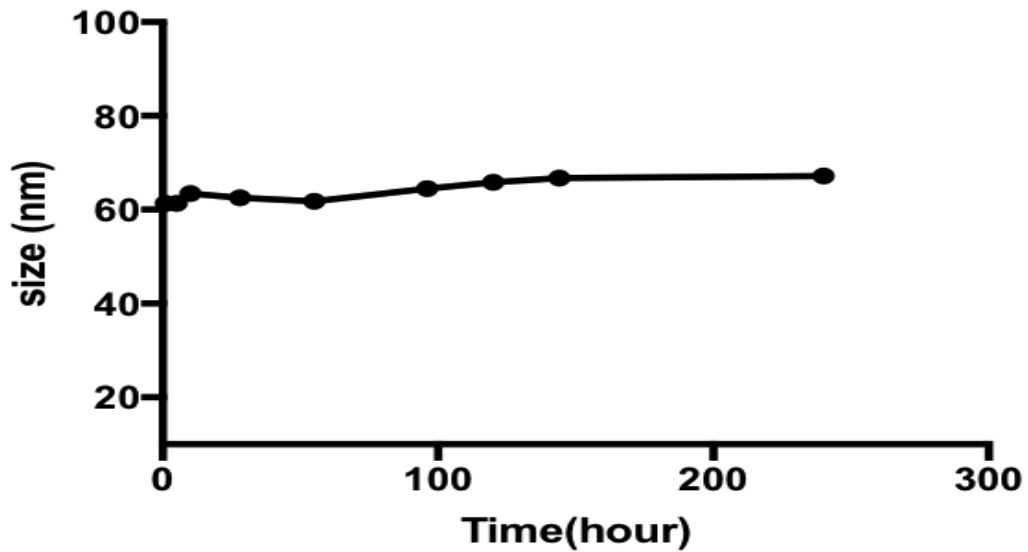


Figure 3.7: The average size of DACHPt-PCCL micelles in the presence of SDS by DLS. DACHPt-PCCL micelles solution (concentration: 1mg/mL) was added to SDS solution (concentration: 6mg/mL) in 2:1 micelles/SDS ratio (n=3).

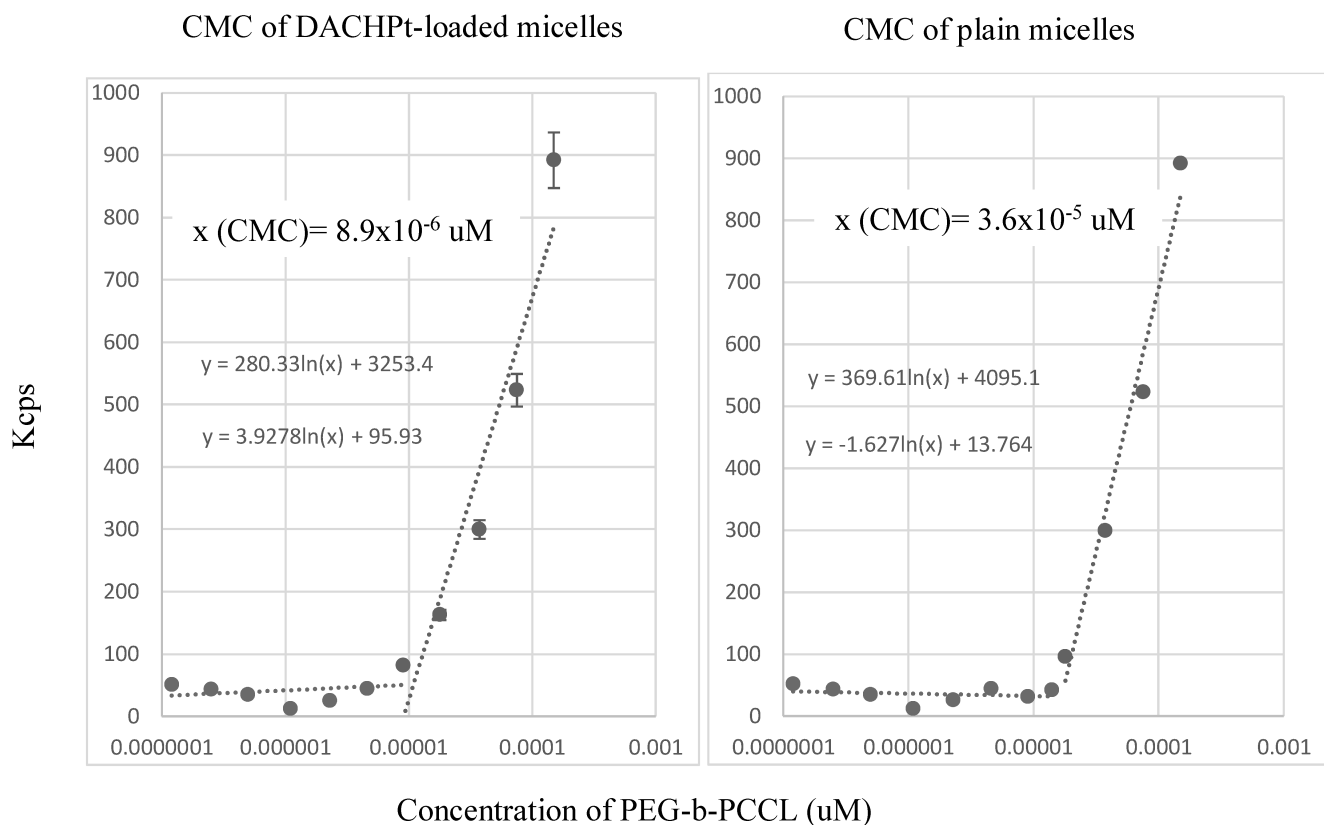


Figure 3.8: Critical micellar concentration CMC of plain and DACHPt-PCCL micelles by DLS (n=3). The equations inserted in the graph represent the linear trend line for the two parts of the sigmoidal graph. The two lines meet at the CMC point.

3.4 *In vitro* drug release

The results of the *in vitro* release of platinum from DACHPt-PCCL micelles compared to the free DACHPt in phosphate buffer pH 7.4 at 37 C° are presented in Figure 3.9. Free DACHPt was released at a rapid rate (90% within 4h). On the other hand, DACHPt-PCCL micelles showed slow and sustained release rate of platinum (only 55 % of platinum was released within 120 h). This means that the transfer of DACHPt through dialysis membrane to the buffer solution is not a restricting factor

and the release of platinum from the micelles is the rate limiting step. The two release profiles were compared using similarity factor f_2 and they were found significantly different from each other ($f_2 = 6.3 < 50$).

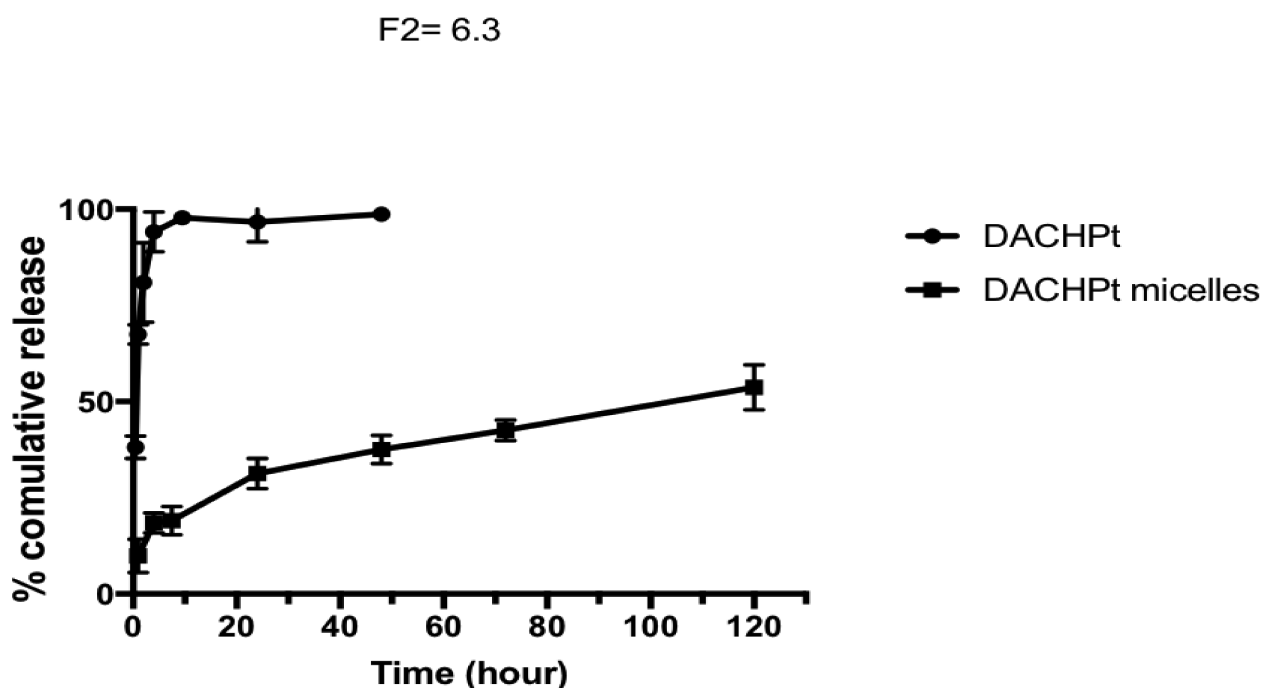
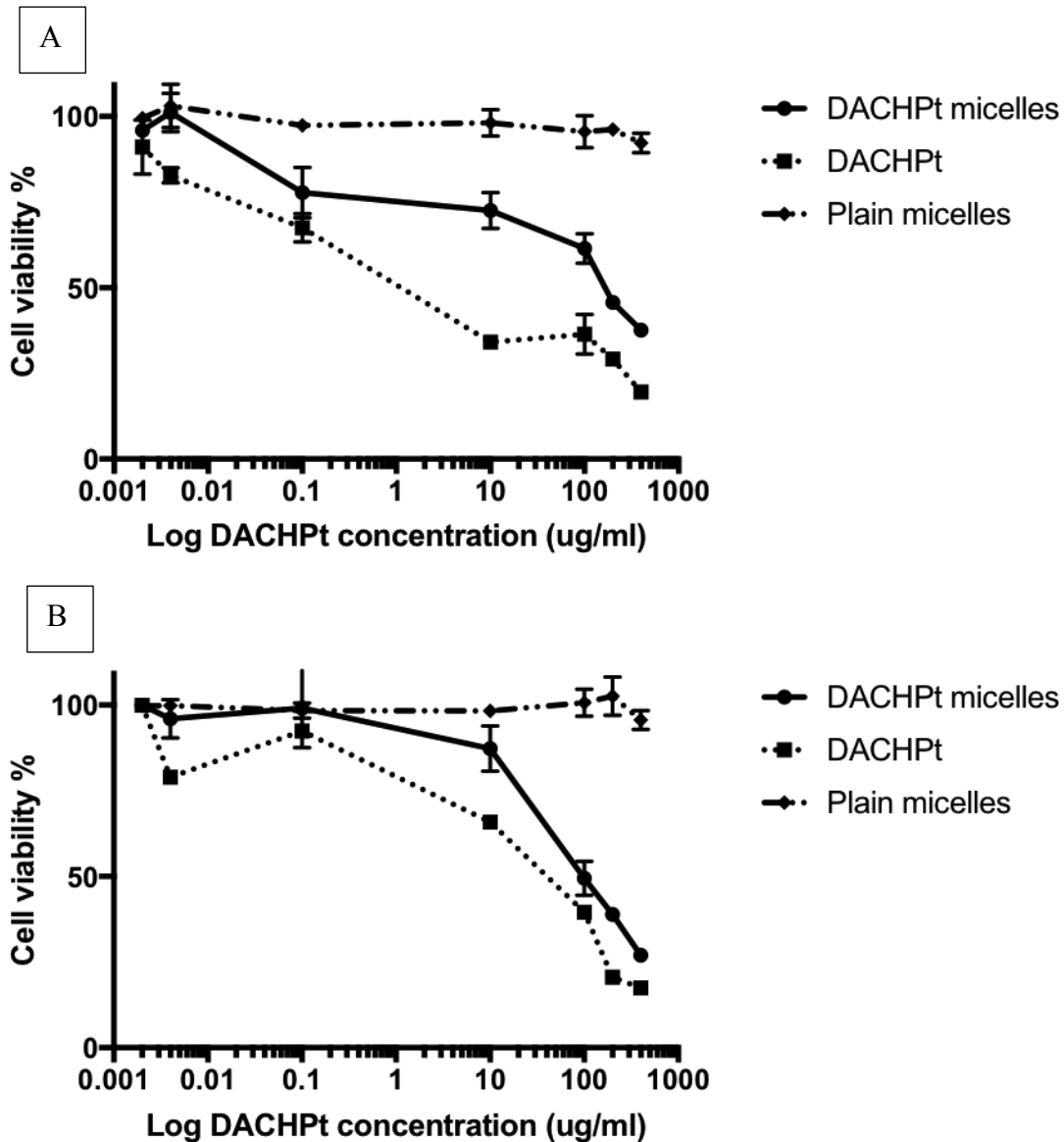


Figure 3.9: In-vitro release profile of platinum from DACHPt-PCCL micelles compared to free DACHPt in PBS (n=3).

3.5 *In vitro* cytotoxicity studies

The cytotoxicity of free DACHPt, DACHPt-PCCL micelles, and PEO-PCCL was assessed using MTT assay. Three human colorectal cancer cell lines (HCT116, SW620, and HT29) were used for these studies. As shown in figure 3.10, the empty micelles showed no cytotoxicity at equivalent concentration on HCT116 cell line

after all incubation times. The cytotoxicity of free DACHPt and DACHPt-PCCL micelles increased as the incubation time increased. As evidenced by higher relative IC₅₀ (Table 3.1). DACHPt-PCCL micelles showed lower cytotoxicity compared to the free DACHPt in all incubation times.



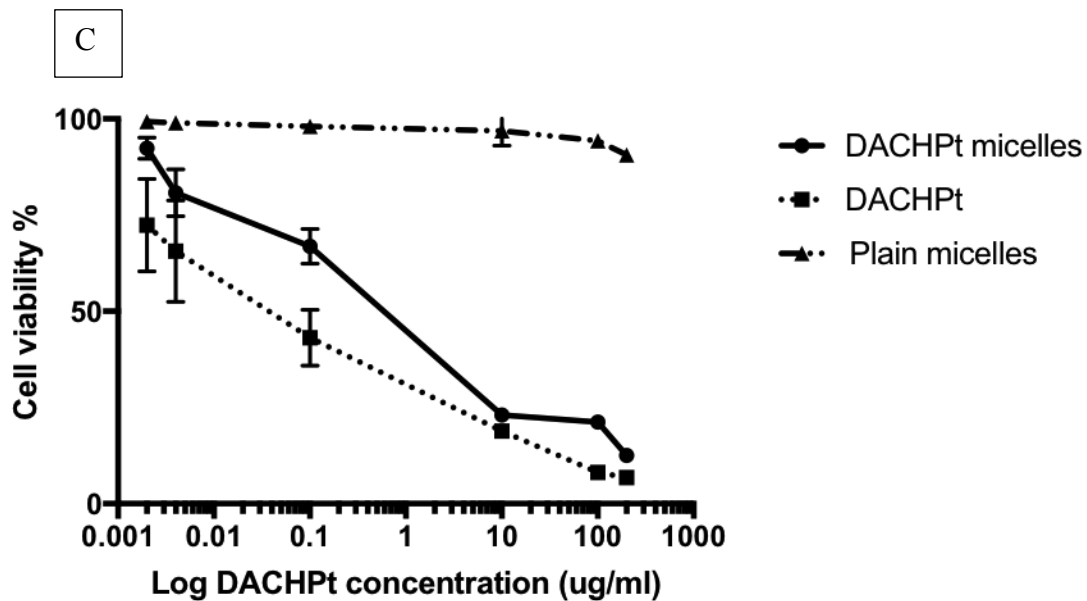
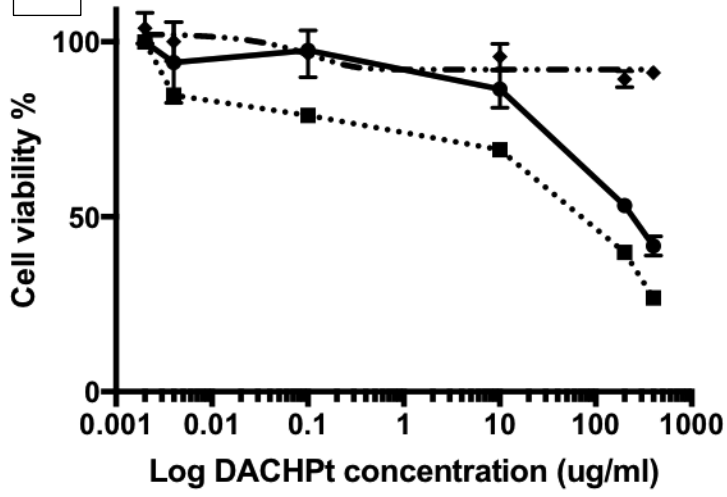


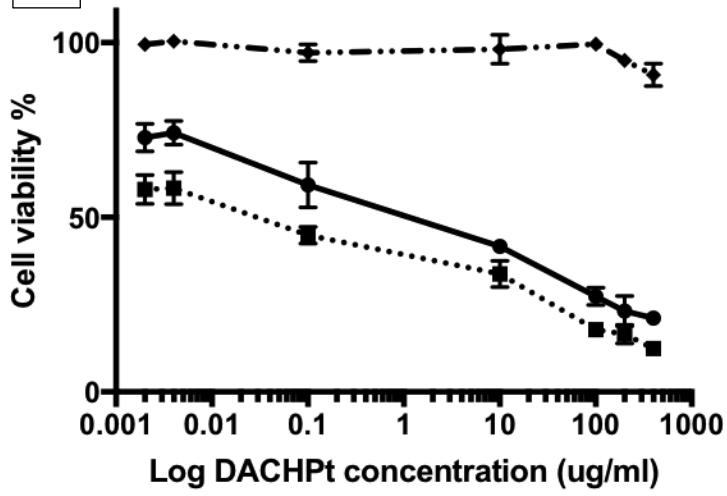
Figure 3.10: Cytotoxicity of DACHPt-PCCL micelles versus control treatments against HCT116 cell line after (A) 24 h, (B) 48 h and (C) 72 h (n=3).

In SW620 cell line, similar results were observed with no cytotoxicity of plain micelles in all the three incubations times. Moreover, SW620 cell line showed a higher sensitivity to DACHPt compared to HCT116 cell line and the cell viability decreased when the time of incubations increased for both free DACHPt and DACHPt-PCCL micelles (Figure 3.11). Higher cytotoxicity was observed in the free DACHPt group compared to DACHPt-PCCL micelles group which resulted in lower IC_{50} for the free DACHPt group in all incubation times (Figure 3.11 and Table 3.1).

A



B



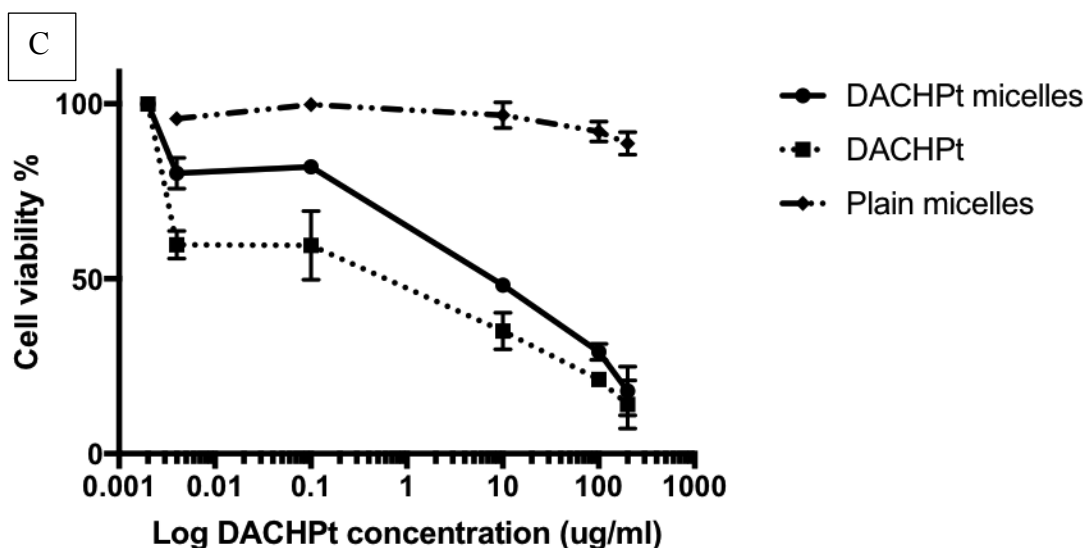
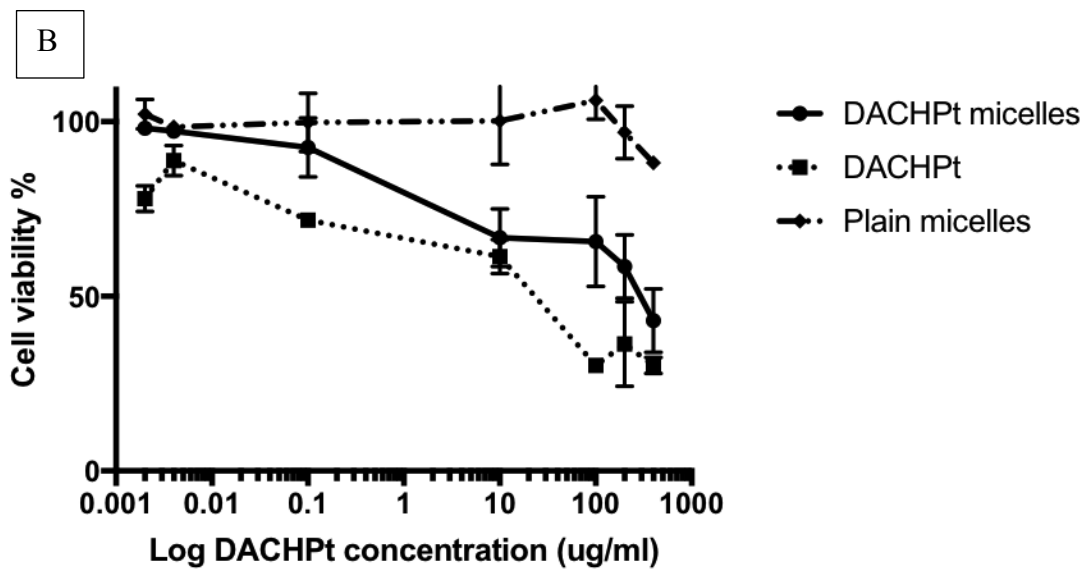
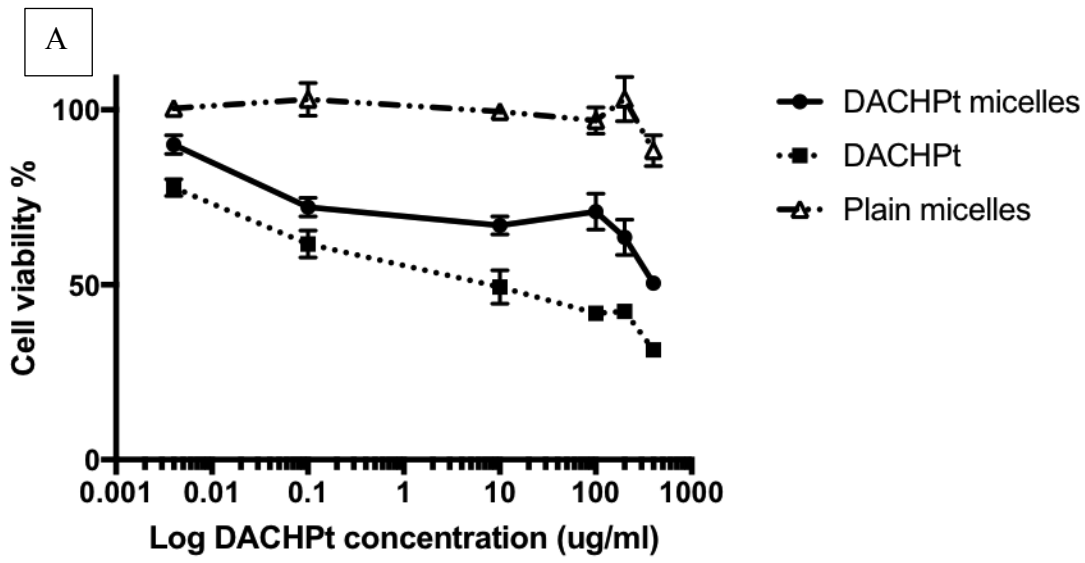


Figure 3.11: Cytotoxicity of DACHPt-PCCL micelles versus control treatments against SW620 cell line after (A) 24 h, (B) 48 h and (C) 72 h (n=3).

HT29 cell line showed lower sensitivity to DACHPt compared to HCT116 and SW620 cell lines. As in HCT116 and SW620 cell lines, the safety of plain micelles was observed in HT29 cell line in all incubation times (Figure 3.12). The results showed an increase in the cytotoxicity of the free DACHPt and DACHPt-PCCL micelles as a result of increasing the incubation time. Free DACHPt showed higher potency than DACHPt-PCCL micelles as evidenced by the lower IC_{50} in all incubation times (Figure 3.12 and Table 3.1). The IC_{50} of the free DACHPt and DACHPt-PCCL micelles in all three cell lines can be shown in Table 3.1.



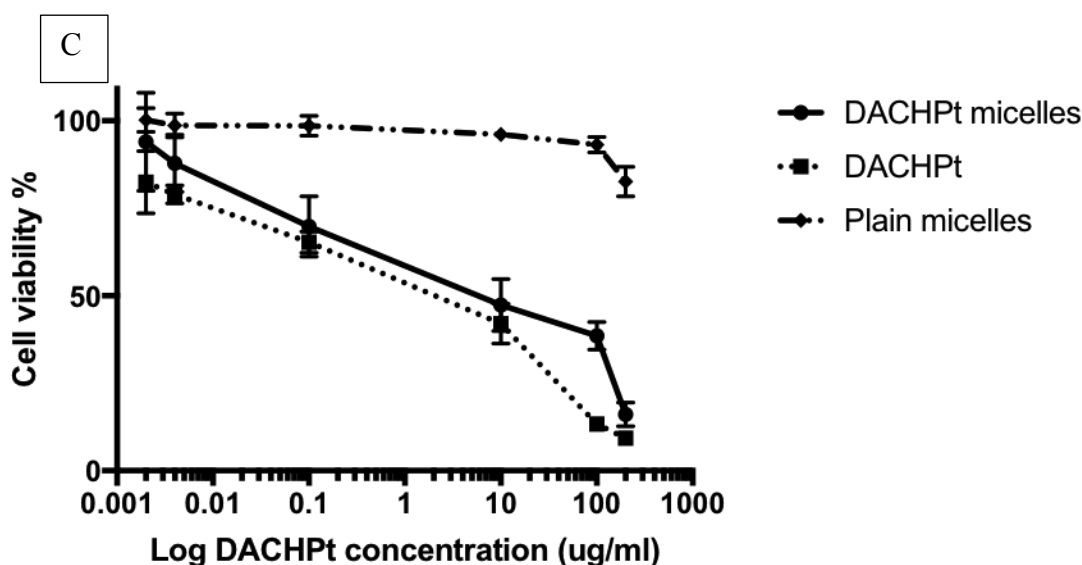


Figure 3.12: Cytotoxicity of DACHPt-PCCL micelles versus control treatments against HT29 cell line after (A) 24 h, (B) 48 h and (C) 72 h (n=3).

Table 3.1: The relative IC₅₀ of DACHPt-PCCL micelles and free DACHPt against HCT116, SW620 and HT29 cell lines after 24, 48 and 72 hours. *Means statistically different from free drug ($P < 0.05$, student's *t*-test), ** means statistically different from free drug ($P < 0.01$, student's *t*-test), **** means statistically different from free drug ($P < 0.0001$, student's *t*-test) under the same conditions. Results are presented as mean \pm SD, n=3.

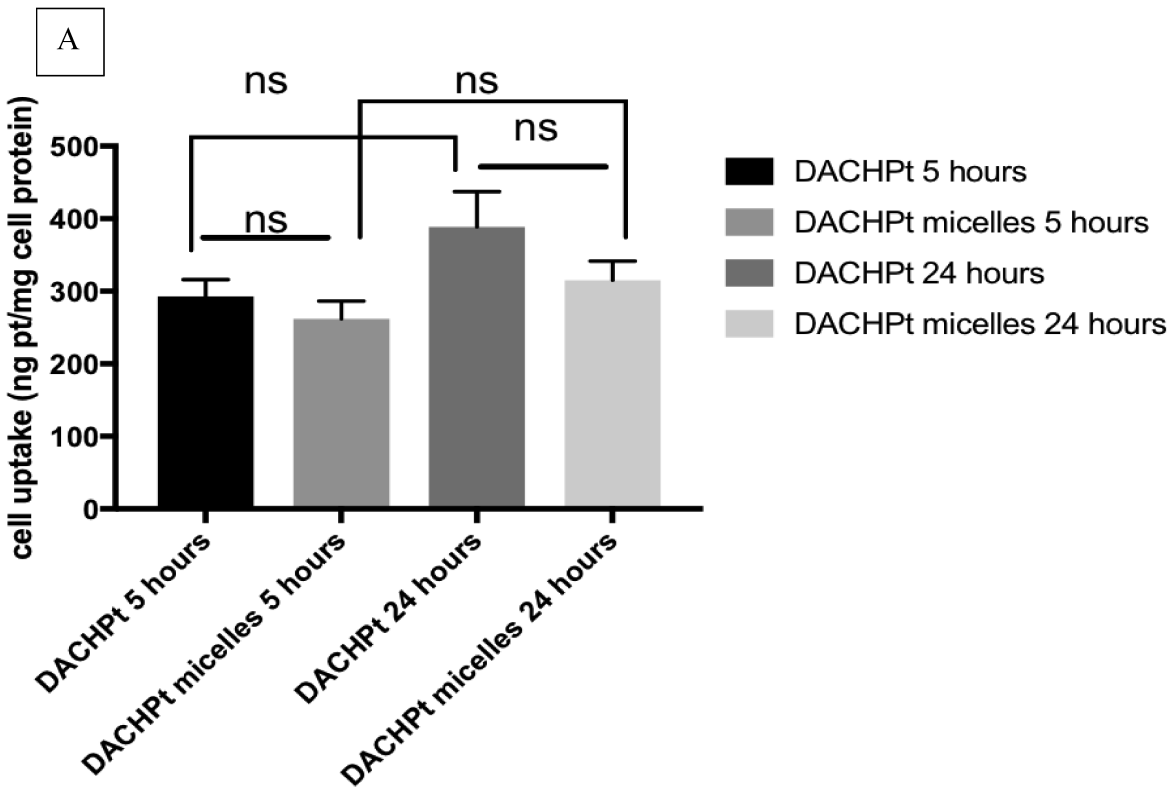
Cell line	Group	IC ₅₀ after 24 h ($\mu\text{g/ml}$)	IC ₅₀ after 48 h ($\mu\text{g/ml}$)	IC ₅₀ after 72 h ($\mu\text{g/ml}$)
HCT116	DACHPt	6.546 \pm 0.743	6.234 \pm 0.793	0.127 \pm 0.09
HCT116	DACHPt micelles	167.7 \pm 6.88****	28.49 \pm 3.134*	2.33 \pm 0.94**
SW620	DACHPt	7.87 \pm 0.39	2.58 \pm 0.29	1.34 \pm 0.19
SW620	DACHPt micelles	214.7 \pm 5.12****	6.07 \pm 0.76*	2.55 \pm 0.09*
HT29	DACHPt	68.38 \pm 5.9	37.49 \pm 4.51	6.859 \pm 0.53
HT29	DACHPt micelles	283.9 \pm 11.32****	176.5 \pm 8.34**	63.22 \pm 3.3****

3.6 *In vitro* cell uptake studies

Cellular uptake of platinum by three human colorectal cancer cell lines (HCT116, SW620, and HT29) was examined through platinum content measurement in the cells after 5 and 24 hours of incubation the cells with free DACHPt or DACHPt-PCCL micelles. In order to quantitatively determine the drug content taken up by the cells, DACHPt and DACHPt-PCCL micelles were incubated with the cells at an equivalent initial platinum concentration. Then, the cells were completely washed and lysed. Platinum content in the cell lysate was determined using ICP-MS. The platinum content is expressed as ng platinum per mg of protein determined by BCA assay (Figure 3.13).

In HCT116 cell line, the uptake of free DACHPt did not increase significantly when incubation time was increased to 24 hours compared to 5 hours ($P>0.05$; Student's *t*-test). Similar observation was made for free drug in SW620 cells. In contrast, in HT29 cells, platinum levels increased as incubation time with free drug was raised to 24h from 5 h ($P< 0.05$, unpaired student's *t* test). Moreover, free DACHPt showed significantly higher cell uptake than DACHPt-PCCL micelles after 24 hours in SW620 cells and after 5 and 24 h in HT29 cells ($P<0.05$; Student's *t*-test). There was no significant increase in the cell uptake of the DACHPt-PCCL micelles at 24 hours compared to after 5 hours ($P>0.05$; Student's *t*-test). There was

no significant increase in the cell uptake of the DACHPt-PCCL micelles compared to free drug at 5 and 24 hours in HCT116 cells ($P>0.05$; Student's t -test). Finally, no time dependence was seen for DACHPt-PCCL micelles in any of the cell lines under study ($P>0.05$, Student's t test).



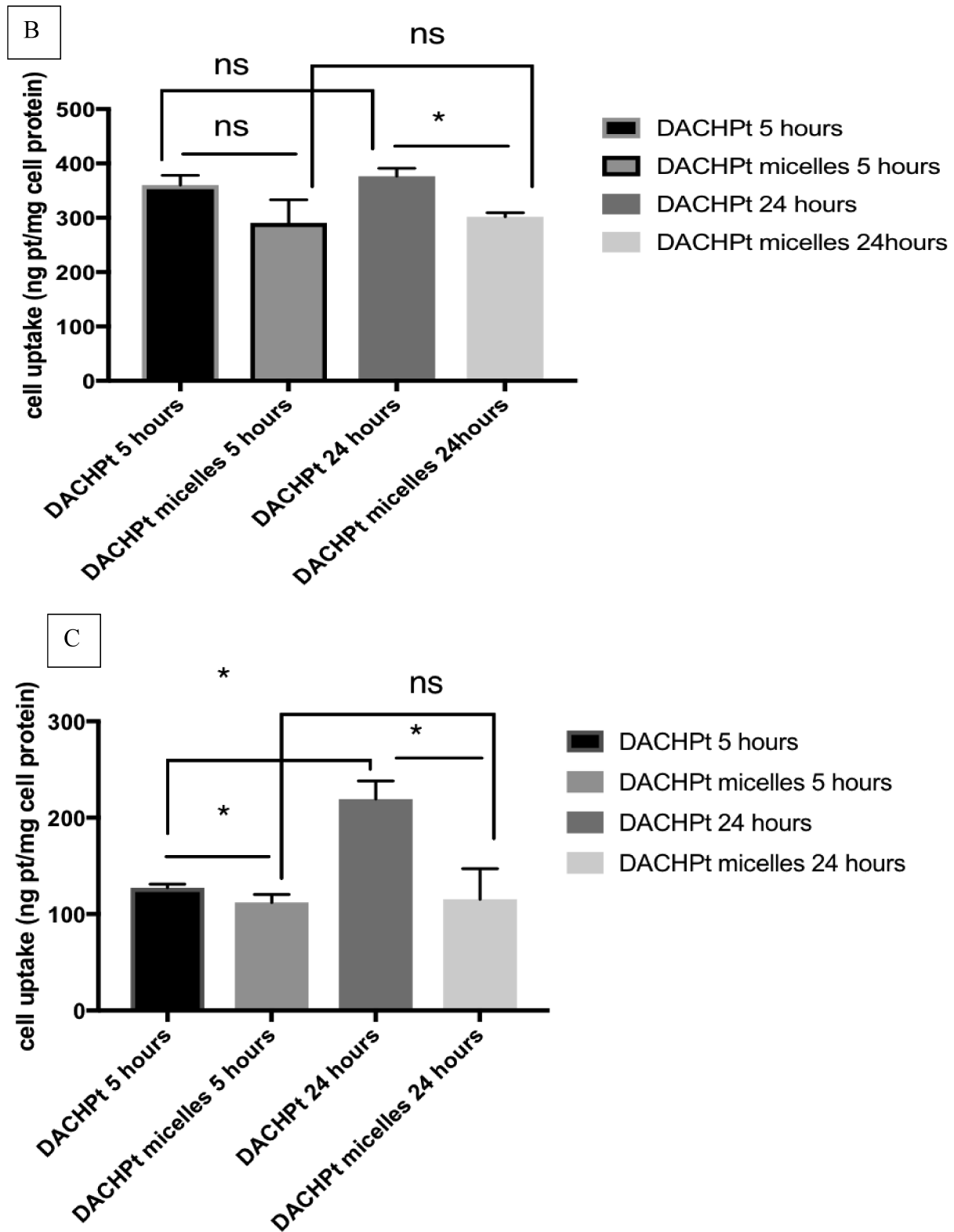
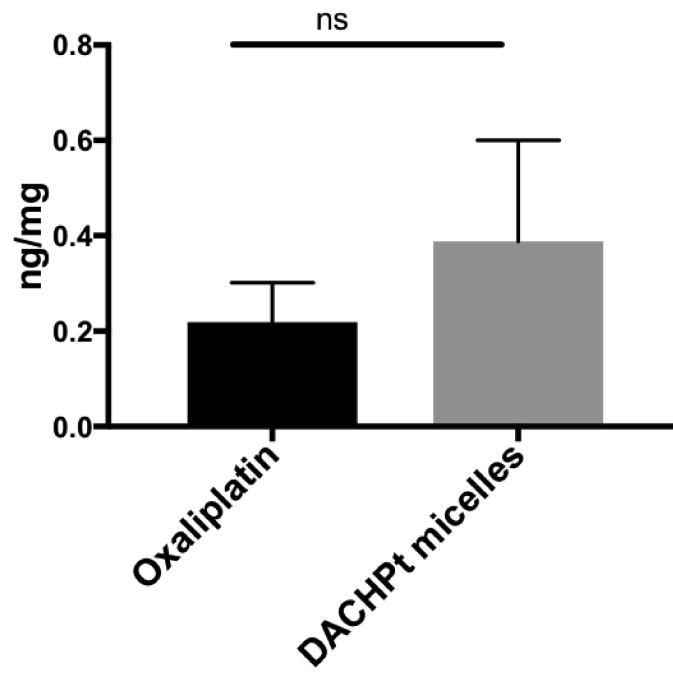


Figure 3.13: Uptake of DACHPt-PCCL micelles versus free DACHPt by (A) HCT116, (B) SW620 and (C) HT29 cells at 5 and 24 hours. *Means statistically different ($P < 0.05$), ns means statistically not different ($P > 0.05$). Each bar represents mean cell uptake \pm SD ($n=3$).

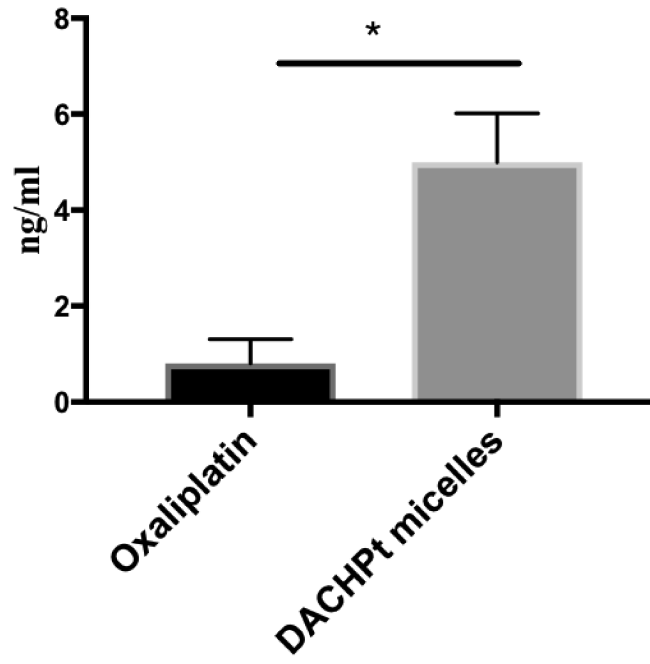
3.7 *In vivo* Biodistribution study

NIH-III mice were inoculated subcutaneously with HCT116 cells to establish tumor xenograft. Mice were divided into two groups (n=3) and injected with oxaliplatin or DACHPt-loaded micelles intravenously in the tail vein at a dose of 6 mg/kg (on a platinum basis). After 24 hours, animals were euthanized, blood was collected, and organs were harvested. Blood and tissue samples were digested, and platinum concentration was determined using ICP-MS. The study revealed that the majority of DACHPt-PCCL micelles were sequestered in the liver and spleen (Figure 3.14). Moreover, higher platinum levels were detected in the plasma in the animals receiving DACHPt-loaded micelles after 24 hours. The accumulation of platinum was detected in all organs tested and ranged from 0.0035 ng/mg tissue in the heart, to 49.4 ng/mg tissue in the liver. A trend for enhanced platinum accumulation in the tumor was observed following administration of DACHPt-PCCL micelles compared to oxaliplatin administration, but the difference was not statistically significant. Drug concentrations were significantly higher in the kidney, liver and spleen of animals that received DACHPt-PCCL micelles group compared to those that received oxaliplatin. In contrast, a trend for higher platinum levels in the brain and lung of animals receiving oxaliplatin was observed compared to those that were injected with DACHPt-PCCL.

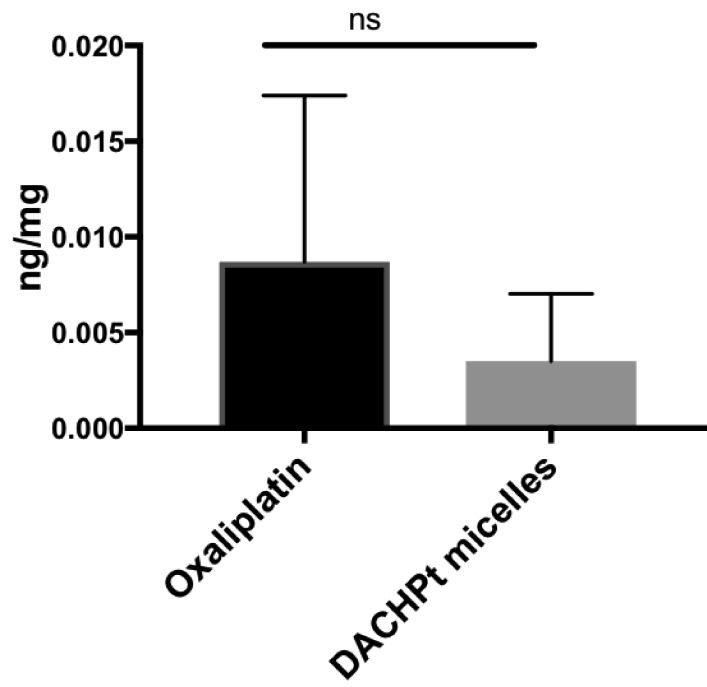
Tumor



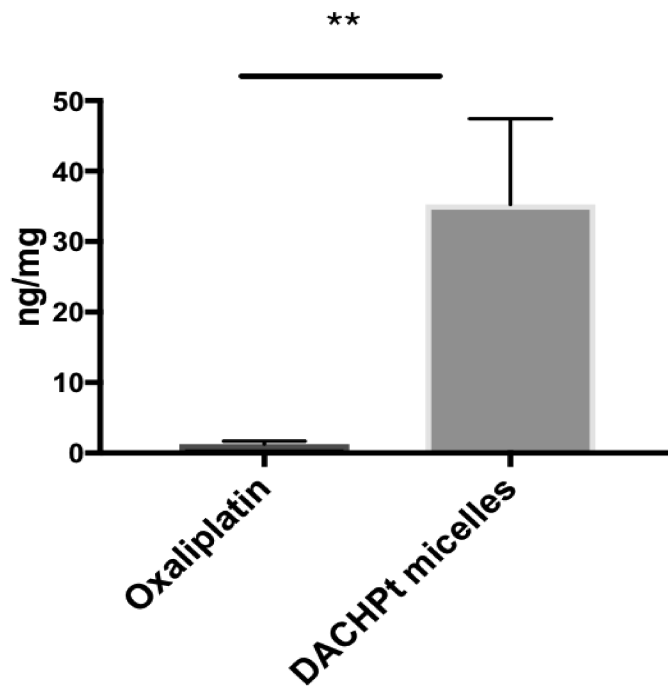
Plasma

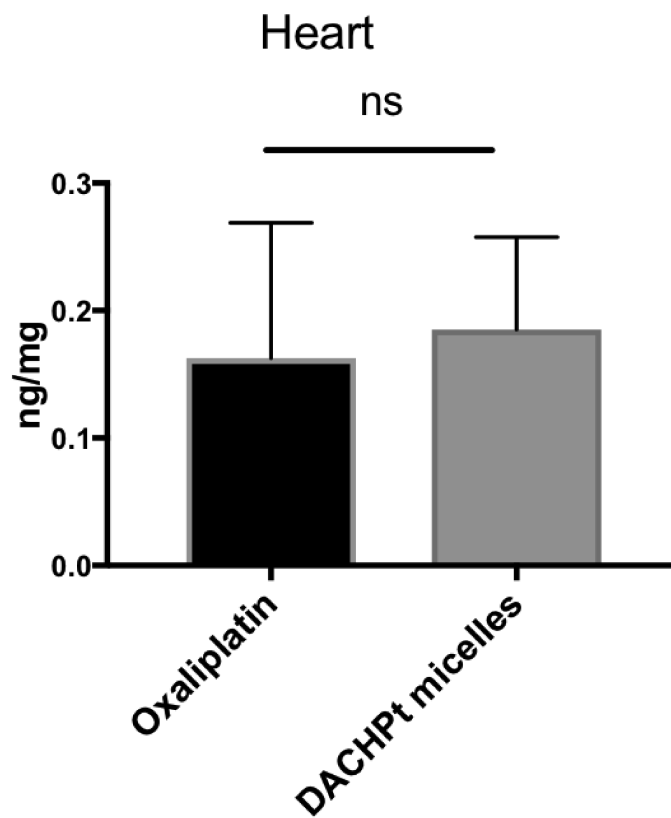
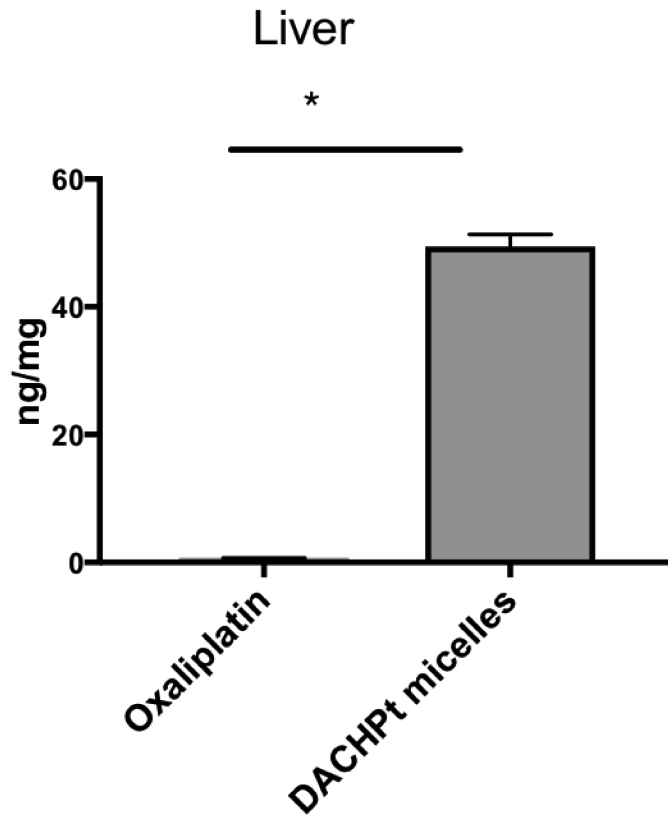


Brain



Spleen





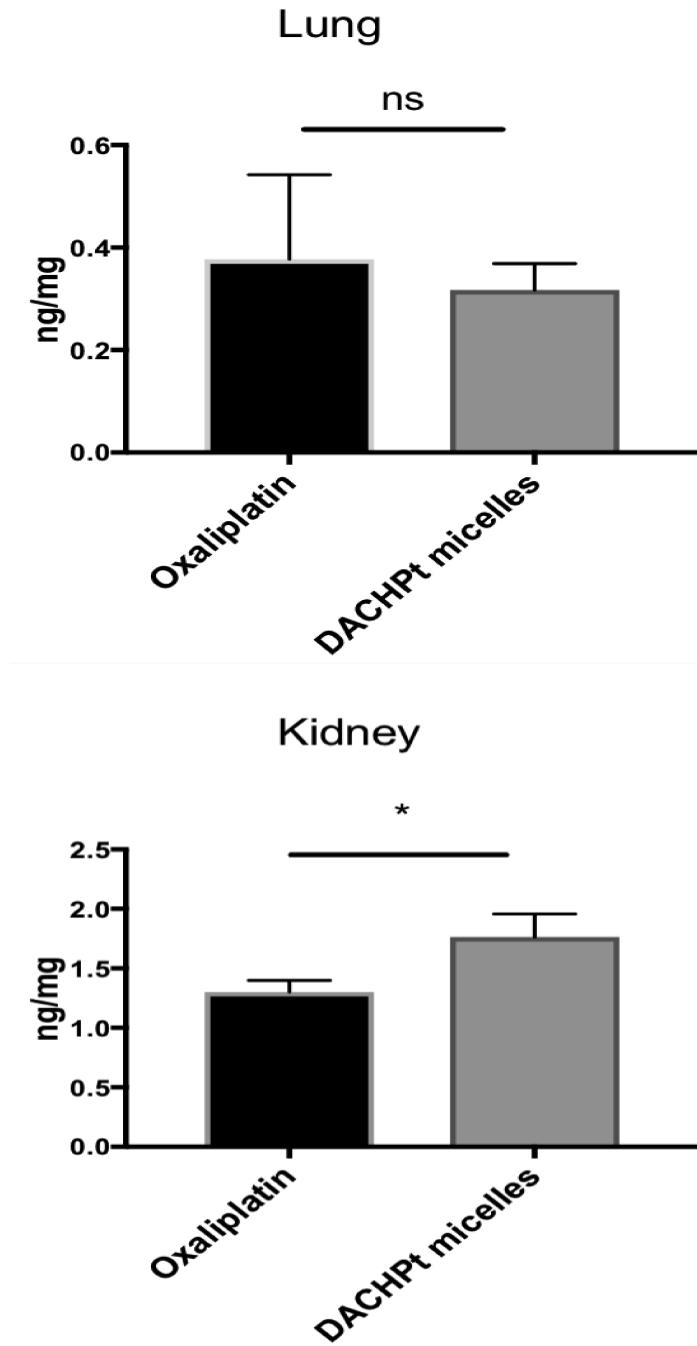


Figure 3.14: Platinum accumulation in organs after 24 hours of injection of oxaliplatin or DACHPt-PCCL micelles intravenously at a dose of 6 mg/kg on a platinum basis. *Means statistically different ($P < 0.05$, students' t test), ns means statistically not different ($P > 0.05$, students' t test). Each bar represents mean platinum accumulation \pm SD (n=3).

The ratio of tissue platinum concentration to the plasma platinum concentration (K_p) of oxaliplatin and DACHPt-PCCL micelles are presented in Table 3.2. The results show significantly higher K_p of platinum following administration of DACHPt-PCCL micelles in liver and spleen compared to free drug, but significantly lower K_p in kidney, lung and heart compared to free drug.

Table 3.2: The ratio of tissue platinum concentration to the plasma platinum concentration (K_p) of oxaliplatin and DACHPt-PCCL micelles. * means statistically different ($P < 0.01$, students, t -test), ns means statistically not different ($P > 0.05$, students' t -test). Results are presented as mean \pm SD (n=3).

Organ	Tumor	Liver	Spleen	Kidney	Lung	Heart	Brain
K_p (Oxaliplatin)	1.08 \pm 1 .15	2.382 \pm 1 .79	6.175 \pm 6 .44	5.9 \pm 5.0 7	1.4 \pm 0.7 6	0.531 \pm 0. 18	0.02 \pm 0.0 4
K_p (DACHPt micelles)	0.207 \pm 0.139 ^{ns}	25.174 \pm 3.94*	18.19 \pm 8 .18*	0.89 \pm 0. 164*	0.16 \pm 0. 02*	0.091 \pm 0. 023*	0.001 \pm 0. 002 ^{ns}

CHAPTER FOUR
DISCUSSION AND CONCLUSION

4.1. Discussion

4.1.1 Development of block copolymer based nanocarriers for DACHPt

The synthesis and characterization of a novel family of self-associating PEO-*b*-PCL based block copolymers carrying pendent benzyl groups on the polyester block (PEO-*b*-PBCL) has previously been reported by our research group [47]. Starting with PEO-*b*-PBCL block copolymer, PEO-*b*-PCCL block copolymer was synthesized through reduction of benzyl carboxylate on the PEO-*b*-PBCL block copolymer. The carboxylic moiety of PEO-*b*-PCCL copolymer makes this copolymer capable of incorporating several drugs or compounds through complex formation and hydrogen bonding [48][49]. Amphiphilic block copolymers like PEO-*b*-PCCL copolymer can self-assemble into various morphologies with different nanostructures [50][51].

The driving force for DACHPt-PCCL micelles assembly is the metal-polymer complex formation between the carboxylic group of the PCCL and the platinum of DACHPt. The average size of DACHPt-PCCL micelles was determined to be 60 nm for the micelles prepared at $[DACHPt]/[PCCL] = 14$. Note that the biodistribution of a colloidal drug carrier and its fate in blood circulation are strongly

affected by the size of the carrier. Removal of many colloidal drug carriers from the blood compartment is due to the recognition by the reticuloendothelial system (RES). The favorable size of a colloidal nanocarrier is below 200 nm to avoid recognition by the RES system and likely, prolong its blood circulation. The hydrophilic PEG that surrounds the core as well as the sub-100 nm size are substantial advantages of the polymeric micelles that can prevent their uptake by the RES leading to longer circulation times in blood. The size of a drug carrier affects its extravasation efficiency critically, and this efficiency varies from tumor to another. This is because diverse pore cutoff sizes are displayed by solid tumors for transvascular transport [52]–[54]. Thus, the size of a drug carrier affects its extravasation efficiency critically, and this efficiency varies from tumor to another. However, the size of DACHPt-PCCL micelles (60 nm) is small enough to expect a high extravasation efficiency regardless of the tumor type [49], [52]. Moreover, deeper penetration into poorly permeable tumors as well as increased accumulation have been reported for carriers with sub-100 sizes [55]. Therefore, the size of DACHPt-PCCL micelles appears to be optimal for tumor-targeted therapy. DACHPt-PCCL micelles showed high encapsulation efficiency EE of 50% and drug loading DL 20% (w/w). DACHPt has a very poor water solubility (0.25 mg/mL). DACHPt-PCCL micelles were able to increase DACHPt solubility to 4.1 mg/mL (i.e. 16 times higher). With this significant increase in water solubility, DACHPt can

be given intravenously at a concentration relevant to the clinically used oxaliplatin infusion solution (5 mg/mL).

Kinetic stability of DACHPt-PCCL micelles in the presence of sodium dodecyl sulfate (SDS), which acted as a micellar destabilizing agent, using DLS by studying the time-dependent changes in the relative scattering light of DACHPt-PCCL micelles. Also, the mean diameter of the micelles was measured by DLS at the same time. SDS has a 12-carbon tail attached to a sulfate group bearing a negative charge that gives the material the amphiphilic properties. When micelles are incubated in the presence of SDS, the straight hydrophobic tail of SDS can adsorb onto the hydrophobic part of the micelles and lead to destabilization of the micelles as a result of the electrostatic repulsion between negatively charged head of SDS [56]. A decrease in the relative scattering intensity of DACHPt-PCCL micelles was considered to be due to a reduction in the molecular weight of the micelles as a result of micellar dissociation. DACHPt-PCCL micelles showed high stability in the presence of SDS and maintained their intensity for 10 days. This high kinetic stability of DACHPt-PCCL micelles could be due to the massive and hydrophobic nature of DACH group in the DACHPt [57]. The higher kinetic stability as well as low CMC (μM levels) of DACHPt-PCCL micelles implies their stability and

retention of the micellar structure upon dilution in blood following intravenous administration of these micelles. The elevated stability of micellar drug carriers in blood is a desired characteristic because it ensures integrity of the micellar structure rather than micellar dissociation that can lead to elimination of block copolymers from kidney filtration. Micellar stability in blood in addition to escape from RES, leads to a longer blood circulation for these nanocarriers. DACHPt-PCCL micelles achieved high kinetic stability, so they seem to be appropriate carrier for prolonged drug circulation that is prerequisite for passive tumor targeting by EPR effect.

A drug carrier should have enough stability to provide a sufficient time for drug delivery to accumulate in the target zone. The stability of polymeric micelles *in vitro* or *in vivo* and their clearance from the body rely on their CMC [58]. The CMC of DACHPt-PCCL and plain micelles were determined by DLS measurement at 25 C° and found to be 8.9×10^{-6} and 3.6×10^{-5} μM , respectively. The scattering intensities detected for DACHPt-PCCL micelles concentrations below CMC have an approximately same value. The intensity starts to show a linear increase with concentration at the CMC, as the number of micelles increases in the solution. CMC is a primary parameter of the thermodynamic stability, it is largely affected by hydrophobic interactions of the amphiphilic polymer [59]. The low CMC of DACHPt-PCCL micelles (8.9×10^{-6} μM) is about 25 times lower than the CMC of low-molecular-mass surfactant micelles like SDS [60]. Moreover, DACHPt-PCCL

micelles showed lower CMC than that of plain PEO-PCCL micelles ($3.6 \times 10^{-5} \mu\text{M}$), and this could be attributed to the complexation between the polymer and the drug. Thus, DACHPt-PCCL micelles can be thermodynamically stable micelles even under highly diluted conditions.

4.1.2 Investigation of DACHPt release from DACHPt-PCCL micelles

When the drug is physically encapsulated in polymeric micelles, the rate of the release is controlled by disintegration of the micelles or by the diffusion of the drug out of the micellar core. However, when the drug is chemically conjugated to the polymer, the drug release happens after the bond between the drug and the polymer has been cleaved [61], [62]. Therefore, when the drug and the polymer form conjugates, the drug release mechanism follow three steps: first, the molecules that break the bond penetrate into the core of the micelles; then, the cleavage of the bonds between polymer and drug occurs; and finally, the drug can diffuse out of the micelles. Another mechanism of drug release is that when the micelles dissociate, the drug is released from individual polymers. Moreover, when the micelles have high stability, the release of the drug can be delayed till the micelles reaches the target. The premature release of the drug from the delivery system is an undesired event, that will reduce the efficiency of targeted drug delivery to diseased site [31].

The release of DACHPT from DACHPt-PCCL micelles was evaluated and compared to the release profile of free DACHPt using equilibrium dialysis method in phosphate buffer (pH 7.4 at 37 C°). Free DACHPt was released from the dialysis bag at a rapid rate (90% within 4h). On the other hand, DACHPt-PCCL micelles showed a slow and sustained release rate of DACHPt and reached only 55 % within 120 h. The release of platinum from the core of the micelles was by exchange reaction between carboxylic groups of PCCL in the platinum complexes and chloride ions in the media (PBS). However, platinum was released from free DACHPt at a rapid rate (90% within 4h). This means that the transfer of platinum through dialysis membrane to buffer solution is not the restricting factor and the release of platinum from the micelles is the rate limiting step. The two release profiles were compared using similarity factor f_2 and the profiles were found to be significantly different ($f_2 = 6.3\% < 50\%$). This unique profile of drug release might be advantageous for *in vivo* use as the drug release is expected to increase after DACHPt-PCCL micelles reach the site of tumor. Although release study was conducted in PBS which has similar chloride level to the blood, the release profile in this study did not show the effect of other factors that are present in the blood, such as plasma proteins, enzymes, blood cells and lipoprotein.

4.1.3 *In-vitro* cell studies

The cytotoxicity of free DACHPt, DACHPt-PCCL micelles, and empty PEO-*b*-PCCL micelles was assessed using MTT assay. Three human colorectal cancer cell lines (HCT116, SW620 and HT29) were used for these studies. In all cell lines, the empty PEO-*b*-PCCL micelles showed no or limited cytotoxicity at equivalent concentrations of that to DACHPt-PCCL micelles at all incubation times (24, 48, and 72 hours). In HCT116 cell line, the cytotoxicity of both free DACHPt and DACHPt-PCCL micelles increased as the incubation time increased. However, DACHPt-PCCL micelles showed lower cytotoxicity compared to the free DACHPt in all incubation times as evidenced by lower IC₅₀. This reduced potency of DACHPt-PCCL micelles is most likely resulted from the slow release of DACHPt from DACHPt-PCCL micelles as no significant difference between Pt levels delivered by free or micellar DACHPt is observed in these cells.

Similarly, In SW620 cell line, the cell viability decreased when the time of incubations increased for both free DACHPt and DACHPt-PCCL micelles. Also, higher cytotoxicity was observed in the free DACHPt group compared to DACHPt-PCCL micelles group which resulted in lower IC₅₀ for the free DACHPt group in all incubation times. This was expected due to the slow release of DACHPt from DACHPt-PCCL micelles, although the higher cellular uptake of DACHPt by

specific cellular transporter (CTR1) in this cell line may have contributed to the higher cytotoxicity of free drug in these cells as well [64]. Besides, SW620 cell line showed higher sensitivity to DACHPt compared to HCT116 cell line. HT29 cell line showed lower sensitivity to DACHPt compared to HCT116 and SW620 cell lines. Similar to HCT116 and SW620 cell lines, the cytotoxicity of the free DACHPt and DACHPt-PCCL micelles increased as a result of increasing the incubation time in HT29 cell line. Moreover, free DACHPt showed higher potency than DACHPt-PCCL micelles as evidenced by reduced IC_{50} . The decreased sensitivity of HT29 over HCT116 and SW620 toward DACHPt could be attributed to lower uptake of DACHPt by HT29 cells.

Free DACHPt is a small molecule that may pass rapidly through the membrane of the cell by diffusion. Moreover, DACHPt like other platinum drugs has specific transporters such as CTR1, and it has been reported that CTR1 increases the accumulation of oxaliplatin in another colorectal cancer cell line [63][64]. However, DACHPt-PCCL micelles delivers its content slowly either by i) slow release of loaded DACHPt from DACHPt-PCCL micelles that gradually diffused through the cell membrane or be taken up by Pt transporters, and/or ii) the cellular uptake of micelles through endocytosis followed by Pt release inside the cell [65]–

[67]. The lower cellular uptake of DACHPt in HT29 cell line after both incubation times could be attributed to the lower expression of platinum transporters on this cell line, but this needs to be investigated.

4.1.5 *In vivo* Biodistribution Study

The major elimination pathway for oxaliplatin is renal clearance. Clinical studies showed that only 15% of the administered dose of platinum was present in the systemic circulation at the end of a 2-h infusion. Ninety % of platinum is irreversibly binds to the plasma protein, and this leads to prevent of oxaliplatin from reaching its target [31]. Moreover, platinum accumulates and irreversibly bind to erythrocyte, so its activity can be diminished [35]. Therefore, an effective delivery system of oxaliplatin could improve its blood circulation. Short-term biodistribution study was performed by an intravenous injection of oxaliplatin or DACHPt-PCCL micelles at a dose of 6 mg pt/kg body weight in tumor bearing mice (n=3). After 24 hours, mice were euthanized, and blood was collected. Organs were harvested, and samples were digested for platinum analysis using ICP-MS. DACHPt-PCCL micelles significantly increased blood platinum levels compared to oxaliplatin. The increased platinum level of DACHPt-PCCL micelles in the bloodstream could be attributed to the high thermodynamic and kinetic stability of DACHPt-PCCL micelles. Moreover, PEG block in DACHPt-PCCL micelles play an important factor

in increasing the platinum level in the blood by providing steric protection against uptake of DACHPt-PCCL micelles by the immune system [55].

It has been reported that an increased accumulation in implanted tumors was observed in PEG-grafted liposomes via EPR effect [68]. However, in some cases, it has also been demonstrated that the use of these liposomes does not have an effect on tumor accumulation [69]. For example, a 100 nm coating liposome did not show an increase in tumor accumulation. This may be attributed to the small cutoff size of the tumor. Thus, drug carriers with smaller size than liposomes may be more efficient for tumor-targeting drug delivery. Here, we have observed that DACHPt-PCCL micelles showed a trend for tumor accumulation of platinum compared to oxaliplatin after 24 hours when compared to platinum levels in tumor by oxaliplatin administration, although the difference was not significant. The higher platinum accumulation by DACHPt-PCCL micelles in tumor is attributed to their high stability of micelles compared to oxaliplatin in blood. The tumor accumulation of platinum delivered by DACHPt-PCCL micelles is expected to further increase after 24 hours compared to platinum delivered by oxaliplatin as at this time the platinum level in the blood in the DACHPt-PCCL micelles group was significantly higher than oxaliplatin. This needs further investigation.

The study revealed that the majority of platinum delivered by DACHPt-PCCL micelles were sequestered in the liver and spleen. This was not surprising as these organs have salient immune functions, but may point to insufficient stealth properties of DACHPt-PCCL micelles developed here. Lower platinum levels were delivered to brain by the micellar formulation compared to oxaliplatin, implying a tendency for lower side effects on the central nervous system by this formulation. Micellar formulation showed significantly lower Kp value in kidney, lung, and heart, but higher Kp value in liver and spleen. These Kp values assure that DACHPt-PCCL micelles are taken up by liver and spleen, and this could be attributed to the elimination of the micelles by RES due to less than optimal stealth effect by PEG. However, DACHPt-PCCL micelles showed lower accumulation in normal tissues (lung, kidney and heart), highlighting the effect of nano-drug delivery in reducing incorporated drug accumulation in normal tissues.

4.2 Conclusion

In this study, methoxy poly(ethylene oxide)-*b*-poly(α -carboxylate- ϵ -caprolactone) (PEO-*b*-PCCL) diblock copolymer was synthesized to prepare micelles complexed with DACHPt. We showed that polymeric nanocarriers of PEO-*b*-PCCL were able to efficiently incorporate DACHPt and increase its water

solubility from 0.25 mg/mL to 4.1 mg/mL (i.e. more than 16 folds). With this significant increase in water solubility, DACHPt can be given intravenously at a concentration relevant to the clinically used in oxaliplatin infusion solution (5 mg/mL). Also, due to the high kinetic stability and lower CMC of DACHPt-PCCL micelles compared to the plain micelles, DACHPt-PCCL micelles showed sustained and significantly slower release profile compared to the free DACHPt. Although DACHPt-PCCL micelles showed lower cytotoxicity than free DACHPt in HCT116 cell line, mainly due to the slow release, similar cellular uptake was found. This means that DACHPt-PCCL micelles can maintain the drug inside the cells, and consequently could facilitate delivering DACHPt to its pharmacological target. In other colorectal cancer cell lines, i.e., SW620 and HT29, a higher IC_{50} and lower Pt cell uptake was mostly observed for the micellar formulation of DACHPt compared to the free drug.

Moreover, the *in vivo* biodistribution study showed a significant increase in blood levels and a trend in tumor accumulation of platinum for DACHPt-PCCL micelles compared to animals injected with oxaliplatin. Despite the positive signs, high liver and spleen Pt accumulation was also found for the micellar formulation of DACHPt compared to oxaliplatin. Overall, the results of this study point to a great potential for DACHPt-PCCL micelles in enhanced delivery of DACHPt to solid tumors. However, there is still a room for improvement of DACHPt-PCCL micelles

to further optimize its biodistribution to decrease the distribution of the drug to normal tissues, especially liver and spleen, and increase its accumulation in the tumor.

4.3 Future directions

While the platinum concentration in plasma at 24 h for DACHPt-PCCL micelles was significantly higher than oxaliplatin, conducting a tissue distribution study for a longer period of time is recommended to investigate whether this high platinum concentration in the blood would lead to a higher tumor accumulation at later time points. Additionally, conducting the *in vivo* biodistribution study considering a larger sample size (i.e. n=5-6 instead of n=3) would provide a better picture of the platinum delivery to different tissues by the micellar formulation over oxaliplatin and decrease the variability in the results making a better case of statistical analysis. Furthermore, a toxicity study needs to be conducted to determine the maximum tolerable dose of micellar DACHPt compared to oxaliplatin and also evaluate the side effects of both formulations on different tissues in mice. Moreover, conducting an efficacy study in tumor-bearing animals would show whether or not DACHPt-PCCL micelles enhance the anti-cancer activity of oxaliplatin in colorectal cancer.

Perhaps the above studies should be accomplished following further optimization of DACHPt-PCCL micelles by changing molecular weight of shell and core-forming block in the micelles to enhance the stealth properties of the PEG shell and as a result, reduce the accumulation of micelles in RES organs, i.e., liver and spleen. It is also preferred if the kinetic stability and release studies can be conducted in an *in vitro* media relevant to the *in vivo* conditions (i.e. plasma or blood). Moreover, further investigation of whether the polymer-metal complex could increase the crosslinking in the core of the micelles, and as a result stability of micelles is warranted. Further studies determining the mechanism of cell interaction and uptake for micellar DACHPt over oxaliplatin will also strengthen the position and conclusions of this study.

References

- [1] S. Dasari and P. B. Tchounwou, "Cisplatin in cancer therapy: molecular mechanisms of action," *Eur. J. Pharmacol.*, vol. 0, pp. 364–378, Oct. 2014.
- [2] M. Galanski, "Recent Developments in the Field of Anticancer Platinum Complexes," *Recent Patents on Anti-Cancer Drug Discovery*, vol. 1, no. 2. pp. 285–295, 2006.
- [3] D. Lebwohl and R. Canetta, "Clinical development of platinum complexes in cancer therapy: an historical perspective and an update," *Eur. J. Cancer*, vol. 34, no. 10, pp. 1522–1534, 1998.
- [4] L. Galluzzi *et al.*, "Molecular mechanisms of cisplatin resistance," *Oncogene*, vol. 31, p. 1869, Sep. 2011.
- [5] G. V Kalayda, C. H. Wagner, and U. Jaehde, "Relevance of copper transporter 1 for cisplatin resistance in human ovarian carcinoma cells," *J. Inorg. Biochem.*, vol. 116, pp. 1–10, 2012.
- [6] D. Kilari, E. Guancial, and E. S. Kim, "Role of copper transporters in platinum resistance," *World J. Clin. Oncol.*, vol. 7, no. 1, pp. 106–113, Feb. 2016.
- [7] J. Zisowsky *et al.*, "Relevance of drug uptake and efflux for cisplatin sensitivity of tumor cells," *Biochem. Pharmacol.*, vol. 73, no. 2, pp. 298–307, 2007.
- [8] A. H. Calvert *et al.*, "Early clinical studies with cis-diammine-1,1-cyclobutane dicarboxylate platinum II," *Cancer Chemother. Pharmacol.*, vol. 9, no. 3, pp. 140–147, Dec. 1982.
- [9] S. Dilruba and G. V. Kalayda, "Platinum-based drugs: past, present and future," *Cancer Chemother. Pharmacol.*, vol. 77, no. 6, pp. 1103–1124, 2016.
- [10] R. F. Ozols *et al.*, "Phase III Trial of Carboplatin and Paclitaxel Compared With Cisplatin and Paclitaxel in Patients With Optimally Resected Stage III Ovarian Cancer: A Gynecologic Oncology Group Study," *J. Clin. Oncol.*, vol. 21, no. 17, pp. 3194–3200, Sep. 2003.
- [11] D. J. Stewart, "Mechanisms of resistance to cisplatin and carboplatin," *Crit. Rev. Oncol. / Hematol.*, vol. 63, no. 1, pp. 12–31, Jul. 2007.
- [12] N. J. Wheate, S. Walker, G. E. Craig, and R. Oun, "The status of platinum anticancer drugs in the clinic and in clinical trials," *Dalt. Trans.*, vol. 39, no. 35, pp. 8113–8127, 2010.
- [13] S. Zhang *et al.*, "Organic Cation Transporters Are Determinants of Oxaliplatin Cytotoxicity," *Cancer Res.*, vol. 66, no. 17, pp. 8847–8857, Sep. 2006.
- [14] A. Tashiro *et al.*, "High expression of organic anion transporter 2 and organic cation transporter 2 is an independent predictor of good outcomes in patients with metastatic colorectal cancer treated with FOLFOX-based chemotherapy," *Am. J. Cancer Res.*, vol. 4, no. 5, pp. 528–536, Sep. 2014.
- [15] E. Martinez-Balibrea *et al.*, "Tumor-Related Molecular Mechanisms of Oxaliplatin Resistance," vol. 14, no. 8, pp. 1767–1776, Aug. 2015.

- [16] E. Wexselblatt and D. Gibson, "What do we know about the reduction of Pt(IV) pro-drugs?," *J. Inorg. Biochem.*, vol. 117, pp. 220–229, 2012.
- [17] H. Maeda, G. Y. Bharate, and J. Daruwalla, "Polymeric drugs for efficient tumor-targeted drug delivery based on EPR-effect," *Eur. J. Pharm. Biopharm.*, vol. 71, no. 3, pp. 409–419, 2009.
- [18] H. S. Oberoi, N. V. Nukolova, A. V. Kabanov, and T. K. Bronich, "Nanocarriers for delivery of platinum anticancer drugs," *Adv. Drug Deliv. Rev.*, vol. 65, no. 13–14, pp. 1667–1685, 2013.
- [19] H. M. Aliabadi and A. Lavasanifar, "Polymeric micelles for drug delivery.," *Expert Opin. Drug Deliv.*, vol. 3, no. 1, pp. 139–162, 2006.
- [20] A. Mahmud, X.-B. Xiong, H. M. Aliabadi, and A. Lavasanifar, "Polymeric micelles for drug targeting," *J. Drug Target.*, vol. 15, no. 9, pp. 553–584, Jan. 2007.
- [21] A. Mahmud, X. B. Xiong, and A. Lavasanifar, "Novel self-associating POly(ethylene oxide)-block-poly(ϵ -caprolactone) block copolymers with functional side groups on the polyester block for drug delivery," *Macromolecules*, vol. 39, no. 26, pp. 9419–9428, 2006.
- [22] X. Zhang, J. K. Jackson, and H. M. Burt, "Development of amphiphilic diblock copolymers as micellar carriers of taxol," *Int. J. Pharm.*, vol. 132, no. 1, pp. 195–206, 1996.
- [23] H. Maeda, "SMANCS and polymer-conjugated macromolecular drugs: advantages in cancer chemotherapy," *Adv. Drug Deliv. Rev.*, vol. 6, no. 2, pp. 181–202, 1991.
- [24] A. M. Jhaveri and V. P. Torchilin, "Multifunctional polymeric micelles for delivery of drugs and siRNA," *Front. Pharmacol.*, vol. 5, p. 77, Apr. 2014.
- [25] T. M. Allen, C. Hansen, F. Martin, C. Redemann, and A. Yau-Young, "Liposomes containing synthetic lipid derivatives of poly(ethylene glycol) show prolonged circulation half-lives in vivo," *Biochim. Biophys. Acta - Biomembr.*, vol. 1066, no. 1, pp. 29–36, 1991.
- [26] G. Gregoriadis, "Liposome research in drug delivery: The early days," *J. Drug Target.*, vol. 16, no. 7–8, pp. 520–524, Jan. 2008.
- [27] J. E. Chung, M. Yokoyama, and T. Okano, "Inner core segment design for drug delivery control of thermo-responsive polymeric micelles," *J. Control. Release*, vol. 65, no. 1, pp. 93–103, 2000.
- [28] A. Lavasanifar, J. Samuel, and G. S. Kwon, "The effect of fatty acid substitution on the in vitro release of amphotericin B from micelles composed of poly(ethylene oxide)-block-poly(N-hexyl stearate-l-aspartamide)," *J. Control. Release*, vol. 79, no. 1, pp. 165–172, 2002.
- [29] Y. Matsumura, "Preclinical and clinical studies of anticancer drug-incorporated polymeric micelles," *J. Drug Target.*, vol. 15, no. 7–8, pp. 507–517, Jan. 2007.
- [30] R. Plummer *et al.*, "A Phase I clinical study of cisplatin-incorporated polymeric micelles (NC-6004) in patients with solid tumours," *Br. J. Cancer*, vol. 104, p. 593, Feb. 2011.
- [31] H. Cabral, N. Nishiyama, S. Okazaki, H. Koyama, and K. Kataoka, "Preparation and biological properties of dichloro(1,2-diaminocyclohexane) platinum(II) (DACHPt)-loaded

- polymeric micelles,” *J. Control. Release*, vol. 101, no. 1–3 SPEC. ISS., pp. 223–232, 2005.
- [32] Y. Kidani, K. Inagaki, M. Iigo, A. Hoshi, and K. Kuretani, “Antitumor activity of 1,2-diaminocyclohexaneplatinum complexes against Sarcoma-180 ascites form,” *J. Med. Chem.*, vol. 21, no. 12, pp. 1315–1318, Dec. 1978.
- [33] O. Rixe *et al.*, “Oxaliplatin, tetraplatin, cisplatin, and carboplatin: Spectrum of activity in drug-resistant cell lines and in the cell lines of the national cancer institute’s anticancer drug screen panel,” *Biochem. Pharmacol.*, vol. 52, no. 12, pp. 1855–1865, 1996.
- [34] C. X. Zhang and S. J. Lippard, “New metal complexes as potential therapeutics,” *Curr. Opin. Chem. Biol.*, vol. 7, no. 4, pp. 481–489, 2003.
- [35] M. A. Graham, G. F. Lockwood, D. Greenslade, S. Brienza, M. Bayssas, and E. Gamelin, “Clinical Pharmacokinetics of Oxaliplatin : A Critical Review Clinical,” *Clin. Cancer Res.*, vol. 18, no. 1, pp. 1205–1218, 2000.
- [36] J. L. Misset, H. Bleiberg, W. Sutherland, M. Bekradda, and E. Cvitkovic, “Oxaliplatin clinical activity: a review.,” *Crit. Rev. Oncol. Hematol.*, vol. 35, no. 2, pp. 75–93, Aug. 2000.
- [37] S. Giacchetti *et al.*, “Phase III multicenter randomized trial of oxaliplatin added to chronomodulated fluorouracil-leucovorin as first-line treatment of metastatic colorectal cancer.,” *J. Clin. Oncol.*, vol. 18, no. 1, pp. 136–147, Jan. 2000.
- [38] J. M. Extra, M. Espie, F. Calvo, C. Ferme, L. Mignot, and M. Marty, “Phase I study of oxaliplatin in patients with advanced cancer.,” *Cancer Chemother. Pharmacol.*, vol. 25, no. 4, pp. 299–303, 1990.
- [39] G. Mathé *et al.*, “Oxalato-platinum or 1-OHP, a third-generation platinum complex: an experimental and clinical appraisal and preliminary comparison with cis-platinum and carboplatinum,” *Biomed. Pharmacother.*, vol. 43, no. 4, pp. 237–250, 1989.
- [40] Y. Xu, Y. Du, H. Yuan, L. Liu, Y. Niu, and F. Hu, “Improved cytotoxicity and multidrug resistance reversal of chitosan based polymeric micelles encapsulating oxaliplatin,” vol. 19, no. May 2010, pp. 344–353, 2011.
- [41] B. Li *et al.*, “A pH responsive complexation-based drug delivery system for oxaliplatin,” *Chem. Sci.*, vol. 8, no. 6, pp. 4458–4464, 2017.
- [42] P.-C. Lee, C.-Y. Lin, C.-L. Peng, and M.-J. Shieh, “Development of a controlled-release drug delivery system by encapsulating oxaliplatin into SPIO/MWNT nanoparticles for effective colon cancer therapy and magnetic resonance imaging,” *Biomater. Sci.*, vol. 4, no. 12, pp. 1742–1753, 2016.
- [43] R. Vivek, R. Thangam, V. Nipunbabu, T. Ponraj, and S. Kannan, “Oxaliplatin-chitosan nanoparticles induced intrinsic apoptotic signaling pathway: A ‘smart’ drug delivery system to breast cancer cell therapy,” *Int. J. Biol. Macromol.*, vol. 65, pp. 289–297, 2014.
- [44] R. K. Dutta and S. Sahu, “Development of oxaliplatin encapsulated in magnetic nanocarriers of pectin as a potential targeted drug delivery for cancer therapy,” *Results Pharma Sci.*, vol. 2, pp. 38–45, 2012.
- [45] A. S. A. Lila, H. Kiwada, and T. Ishida, “Selective Delivery of Oxaliplatin to Tumor

- Tissue by Nanocarrier System Enhances Overall Therapeutic Efficacy of the Encapsulated Oxaliplatin,” *Biol. Pharm. Bull.*, vol. 37, no. 2, pp. 206–211, 2014.
- [46] Y. Mochida, H. Cabral, and K. Kataoka, “Polymeric micelles for targeted tumor therapy of platinum anticancer drugs,” *Expert Opin. Drug Deliv.*, vol. 14, no. 12, pp. 1423–1438, 2017.
- [47] A. Mahmud, X.-B. Xiong, and A. Lavasanifar, “Novel Self-Associating Poly(ethylene oxide)-block-poly(ϵ -caprolactone) Block Copolymers with Functional Side Groups on the Polyester Block for Drug Delivery,” *Macromolecules*, vol. 39, no. 26, pp. 9419–9428, Dec. 2006.
- [48] M. Shahin, N. Safaei-Nikouei, and A. Lavasanifar, “Polymeric micelles for pH-responsive delivery of cisplatin,” *J. Drug Target.*, vol. 22, no. 7, pp. 629–637, 2014.
- [49] H. Cabral *et al.*, “Accumulation of sub-100 nm polymeric micelles in poorly permeable tumours depends on size,” *Nat. Nanotechnol.*, vol. 6, no. 12, pp. 815–823, 2011.
- [50] C. Fetsch, J. Gaitzsch, L. Messenger, G. Battaglia, and R. Luxenhofer, “Self-Assembly of Amphiphilic Block Copolypeptides – Micelles, Worms and Polymersomes,” *Sci. Rep.*, vol. 6, p. 33491, Sep. 2016.
- [51] L. Zhang and A. Eisenberg, “Multiple Morphologies and Characteristics of ‘Crew-Cut’ Micelle-like Aggregates of Polystyrene-*b*-poly(acrylic acid) Diblock Copolymers in Aqueous Solutions,” *J. Am. Chem. Soc.*, vol. 118, no. 13, pp. 3168–3181, Jan. 1996.
- [52] S. K. Hobbs *et al.*, “Regulation of transport pathways in tumor vessels: Role of tumor type and microenvironment,” *Proc. Natl. Acad. Sci. U. S. A.*, vol. 95, no. 8, pp. 4607–4612, Apr. 1998.
- [53] O. Ishida, K. Maruyama, K. Sasaki, and M. Iwatsuru, “Size-dependent extravasation and interstitial localization of polyethyleneglycol liposomes in solid tumor-bearing mice,” *Int. J. Pharm.*, vol. 190, no. 1, pp. 49–56, 1999.
- [54] Y. Matsumura and H. Maeda, “A new concept for macromolecular therapeutics in cancer chemotherapy: mechanism of tumoritropic accumulation of proteins and the antitumor agent smancs.,” *Cancer Res.*, vol. 46, no. 12 Pt 1, pp. 6387–6392, Dec. 1986.
- [55] N. Anatoly and P. Vladimir, “Polyethylene glycol-diacyllipid micelles demonstrate increased ...,” vol. 19, no. 10, pp. 1424–1429, 2002.
- [56] A. Kellarakis, C. Chaibundit, M. J. Krysmann, V. Havredaki, K. Viras, and I. W. Hamley, “Interactions of an anionic surfactant with poly(oxyalkylene) copolymers in aqueous solution,” *J. Colloid Interface Sci.*, vol. 330, no. 1, pp. 67–72, 2009.
- [57] J. A. Platts, D. E. Hibbs, T. W. Hambley, and M. D. Hall, “Calculation of the Hydrophobicity of Platinum Drugs,” *J. Med. Chem.*, vol. 44, no. 3, pp. 472–474, Feb. 2001.
- [58] V. P. Torchilin, “Structure and design of polymeric surfactant-based drug delivery systems,” *J. Control. Release*, vol. 73, no. 2, pp. 137–172, 2001.
- [59] S. C. Owen, D. P. Y. Chan, and M. S. Shoichet, “Polymeric micelle stability,” *Nano Today*, vol. 7, no. 1, pp. 53–65, 2012.
- [60] F. Bian, L. Jia, W. Yu, and M. Liu, “Self-assembled micelles of N-phthaloylchitosan-g-

- polyvinylpyrrolidone for drug delivery,” *Carbohydr. Polym.*, vol. 76, no. 3, pp. 454–459, 2009.
- [61] C. Allen, D. Maysinger, and A. Eisenberg, “Nano-engineering block copolymer aggregates for drug delivery,” *Colloids Surfaces B Biointerfaces*, vol. 16, no. 1, pp. 3–27, 1999.
- [62] A. Lavasanifar, J. Samuel, and G. S. Kwon, “Poly(ethylene oxide)-block-poly(l-amino acid) micelles for drug delivery,” *Adv. Drug Deliv. Rev.*, vol. 54, no. 2, pp. 169–190, 2002.
- [63] S. B. Howell, R. Safaei, C. A. Larson, and M. J. Sailor, “Copper Transporters and the Cellular Pharmacology of the Platinum-Containing Cancer Drugs,” *Mol. Pharmacol.*, vol. 77, no. 6, pp. 887–894, Jun. 2010.
- [64] P. Noordhuis, A. C. Laan, K. van de Born, N. Losekoot, I. Kathmann, and G. J. Peters, “Oxaliplatin activity in selected and unselected human ovarian and colorectal cancer cell lines,” *Biochem. Pharmacol.*, vol. 76, no. 1, pp. 53–61, 2008.
- [65] T. Hamaguchi *et al.*, “A phase I and pharmacokinetic study of NK105, a paclitaxel-incorporating micellar nanoparticle formulation,” *Br. J. Cancer*, vol. 97, p. 170, Jun. 2007.
- [66] K. Chin *et al.*, “Phase II study of NK105, a paclitaxel-incorporating micellar nanoparticle as second-line treatment for advanced or recurrent gastric cancer.,” *J. Clin. Oncol.*, vol. 28, no. 15_suppl, p. 4041, May 2010.
- [67] G. Yang, J. Wang, D. Li, and S. Zhou, “Polyanhydride micelles with diverse morphologies for shape-regulated cellular internalization and blood circulation,” *Regen. Biomater.*, vol. 4, no. 3, pp. 149–157, Jun. 2017.
- [68] D. Papahadjopoulos *et al.*, “Sterically stabilized liposomes: improvements in pharmacokinetics and antitumor therapeutic efficacy,” *Proc. Natl. Acad. Sci.*, vol. 88, no. 24, p. 11460 LP-11464, Dec. 1991.
- [69] M. J. Parr, D. Masin, P. R. Cullis, and M. B. Bally, “Accumulation of Liposomal Lipid and Encapsulated Doxorubicin in Murine Lewis Lung Carcinoma: The Lack of Beneficial Effects by Coating Liposomes with Poly(ethylene glycol),” *J. Pharmacol. Exp. Ther.*, vol. 280, no. 3, p. 1319 LP-1327, Mar. 1997.